

Drag and thermophoresis on a sphere in a rarefied gas based on the Cercignani-Lampis model of gas-surface interaction

Denize Kalempa^{1†} and Felix Sharipov²

¹Departamento de Ciências Básicas e Ambientais, Escola de Engenharia de Lorena,
Universidade de São Paulo, 12602-810, Lorena, Brazil

²Departamento de Física, Universidade Federal do Paraná, Caixa Postal 19044, 81531-990,
Curitiba, Brazil

(Received xx; revised xx; accepted xx)

In the present work, the influence of the gas-surface interaction law on the classical problems of viscous drag and thermophoresis on a spherical particle with high thermal conductivity immersed in a monatomic rarefied gas is investigated on the basis of the solution of a kinetic model to the linearized Boltzmann equation. The scattering kernel proposed by Cercignani and Lampis is employed to model the gas-surface interaction law via the setting of two accommodation coefficients, namely the tangential momentum accommodation coefficient (TMAC) and the normal energy accommodation coefficient (NEAC). The viscous drag and thermophoretic forces acting on the sphere are calculated in a wide range of the rarefaction parameter, which is defined as the ratio of the sphere radius to an equivalent free path of gaseous particles, so that the free molecular, transition and continuum regimes of the gas flow are covered. In the free molecular regime the problem is solved analytically via the method of the characteristics to solve the collisionless kinetic equation, while in the transition and continuum regimes the discrete velocity method is employed to solve the kinetic equation numerically. The numerical calculations are carried out in a range of accommodation coefficients which covers most situations encountered in practice. The macroscopic characteristics of the gas flow around the sphere, namely the density and temperature deviations from thermodynamic equilibrium far from the sphere, the bulk velocity and the heat flux are calculated and their profiles as functions of the radial distance from the sphere are presented for some values of rarefaction parameter and accommodation coefficients. The results show the appearance of the negative thermophoresis in the near continuum regime and the dependence of this phenomenon on the accommodation coefficients. To verify the reliability of the calculations, the reciprocity relation between the cross phenomena which is valid at arbitrary distance from the sphere was found and then verified numerically within an accuracy of 0.1%. The results for the thermophoretic force are compared to the more recent experimental data found in the literature for a copper sphere in argon gas.

1. Introduction

Problems regarding viscous drag and thermophoresis on spherical particles immersed in a rarefied gas are classical in the field of rarefied gas dynamics and have been investigated by many authors over the years, see e.g. Yamamoto & Ishihara (1988); Takata & Sone (1992); Loyalka (1992); Beresnev & Chernyak (1995); Takata & Sone

† Email address for correspondence: kalempa@usp.br

(1995); Chernyak & Sogradi (2019). The study of this topic is motivated by its fundamental importance for the understanding of the physics underlying some phenomena, such as the transport of aerosols in the atmosphere, and for practical applications such as the development of technologies in the fields of microfluidics, semiconductor industry, security of nuclear plants, etc. The well known equations of continuum mechanics, namely the Navier-Stokes-Fourier equations, see e.g. Landau & Lifshitz (1989), can be used to calculate the drag and the thermophoretic forces acting on a sphere, as well as the macroscopic characteristics of the gas flow around it, only in situations where the molecular mean free path is significantly smaller than a characteristic length of the gas flow domain so that the continuum hypothesis is still valid. The Knudsen number (Kn), defined as the ratio of the molecular mean free path to a characteristic length of the gas flow, is the parameter often used to classify the gas flow regimes. The equations of continuum mechanics are valid when $Kn \ll 1$. For instance, in air at standard conditions, the molecular mean free path is approximately $0.065 \mu\text{m}$. Then, for small particles originated from several sources moving through the air, the Knudsen number varies from about zero to 65 when the size of particles ranges from $100 \mu\text{m}$ to $10^{-3} \mu\text{m}$. Therefore, the modelling of the gas flow around aerosols in the atmosphere, as well as the movement of these particles itself, cannot be accurately described by the equations of continuum mechanics. Moreover, even in the continuum regime, the Navier-Stokes-Fourier equations cannot predict the negative thermophoresis, which means the movement of aerosol particles from cold to hot regions. This phenomenon was first predicted theoretically by Sone (1972) for aerosol particles with high thermal conductivity related to that of the carrier gas. However, experimental data regarding this phenomenon is still scarce in the literature because its detection is very difficult. Actually, the more recent data concerning negative thermophoresis is provided by Bosworth *et al.* (2016), in which the thermophoretic force on a copper sphere in argon gas was measured in a wide range of the gas rarefaction.

Historically, the viscous drag force on a sphere was first investigated by Stokes (1845) via hydrodynamic analysis based on the Navier-Stokes-Fourier equations, with the derivation of his famous formula for the drag force on a sphere in a slow flow, see e.g. Landau & Lifshitz (1989). Regarding the thermophoresis, the first attempt to calculate the thermal force on a sphere in a gas with a temperature gradient was done by Epstein (1924). Since the theories of both Stokes and Epstein were valid in the continuum regime, many attempts to modify the equations of continuum mechanics as well as the boundary conditions were proposed over the years to increase their range of applicability in the Knudsen number. For instance, the correction factor proposed by Cunningham (1910) to consider the non-continuum effects of gas slippage on the boundary was incorporated in the Stokes formula so that its applicability was extended to the so called slip flow regime. Concerning the thermophoresis, continuum analysis based on the Navier-Stokes-Fourier equations with slip corrections in the boundary condition was first carried out by Brock (1962) in an attempt to improve the previous theory proposed by Epstein. Methods based on the use of higher-order kinetic theory approximations, as that first proposed by Grad (1949), were also employed to solve the problems of drag and thermophoresis on a sphere. For instance, Sone (1972) obtained an expression for the thermophoretic force acting on a sphere with uniform temperature corrected up to the second order in the Knudsen number using an asymptotic theory for small Knudsen numbers and predicted the negative thermophoresis. In a more recent paper, Torrilhon (2010) investigated a slow flow past a sphere on the basis of the regularized 13-moment equations as proposed by Struchtrup & Torrilhon (2003), a method which relies on the combination of the moment approximation and asymptotic expansion in kinetic theory of gases. Similarly,

Padrino *et al.* (2019) investigated the thermophoresis on a sphere by employing the same method and predicted the negative thermophoresis. According to Torrillon (2010) and Padrino *et al.* (2019), the regularized 13-moment method can be used to describe the drag and the thermophoresis on a sphere when $Kn < 1$. In fact, although many efforts have been done over the years to expand the validity of the continuum models in the description of gas flows, it is well known that all the theories and methods currently available fail in describing gas flows properly when $Kn \sim 1$ or $Kn \gg 1$. In these kinds of situations, corresponding to transition and free molecular regimes, the problem must be solved at the microscopic level via the methods of rarefied gas dynamics, which are based on either the solution of the Boltzmann equation, see e.g. Cercignani (1988); Sharipov (2016), and its related kinetic models, e.g. Bhatnagar *et al.* (1954); Shakhov (1968), or the Direct Simulation Monte Carlo method as pioneered by Bird (1994).

Although an extensive literature concerning the topic under investigation in the whole range of the Knudsen number based on kinetic theory is available, most of the papers rely on the assumption of diffuse reflection or complete accommodation of gas molecules on the surface, see e.g. the reviews on thermophoresis by Zheng (2002) and Young (2011). However, in practice, the assumption of complete accommodation of gas molecules on the surface is not always valid and its use can lead to large deviations of theoretical predictions from experimental data. As pointed out by Zheng (2002), actually the gas-surface interaction law is most probably something between the widely used diffuse and specular reflection models. Thus, the so called accommodation coefficients on the surface should be conveniently introduced to accurately describe the gas-surface interaction. From our knowledge, Beresnev & Chernyak (1995); Beresnev *et al.* (1990) were the first authors to study the influence of the gas-surface interaction law on the drag and thermophoretic forces acting on a sphere with basis on a kinetic model to the Boltzmann equation in the whole range of the Knudsen number. These authors solved the linearized kinetic equation proposed by Shakhov (1968) numerically via the integral-moment method, with boundary condition written in terms of accommodation coefficients of momentum and energy as proposed by Shen (1967), with the distribution function of reflected molecules from the surface approximated by an expansion in terms of Hermite polynomials and unknown accommodation coefficients determined from the conservation laws of momentum and energy on the particle surface. The qualitative results presented by the authors show a strong dependence of the drag and thermophoretic forces on the accommodation coefficients.

Currently, the scattering kernel proposed by Cercignani & Lampis (1971) is considered the most reliable to model the gas-surface interaction law because it provides a correct physical description of many transport phenomena in gases which are not described correctly by other models of gas-surface interaction available in the literature. For instance, several experimental data show us that the exponent which appear in the thermomolecular pressure difference at low pressures varies from 0.4 to 0.5, see e.g. Podgursky & Davis (1961); Edmonds & Hobson (1965). However, as pointed out by Sharipov (2003*b*), the widely used diffuse-specular model proposed by Maxwell for the gas-surface interaction cannot explain the reason for the deviation of such exponent from 0.5 in the free molecular regime. On the contrary, the model proposed by Cercignani-Lampis provides a more correct description of this phenomenon. Concerning the problem of thermophoresis and drag on a sphere, the results presented recently by Chernyak & Sograb (2019) in the free molecular regime show a qualitative disagreement between the values of forces obtained from different scattering kernels. As pointed out by the authors, since all the experimental data available in the literature were obtained for small and intermediate Knudsen number, experiments in the free molecular regime

should be carried out to verify which model is closer to reality. In the Cercignani-Lampis model of gas-surface interaction, two independent accommodation coefficients are introduced, namely the tangential momentum accommodation coefficient (TMAC) and the normal energy accommodation coefficient (NEAC). This model assumes that the NEAC ranges from 0 to 1, while the TMAC ranges from 0 to 2. In practice, the values of these accommodation coefficients extracted from experiments can be found in the literature, see e.g. Semyonov *et al.* (1984); Trott *et al.* (2011); Sazhin *et al.* (2001); Sharipov & Moldover (2016) for several gases and surfaces. For instance, according to Trott *et al.* (2011); Sharipov & Moldover (2016), the NEAC ranges from 0 to 0.1 for Helium and from 0.5 to 0.95 for Argon at ambient temperature and several different smooth metallic surfaces such as aluminum, platinum and stainless steel. Moreover, the TMAC of Helium and Argon ranges from 0.5 to 1 at the same conditions. According to the results presented by Chernyak & Sograbi (2019), in the free molecular regime the Cercignani-Lampis model leads the thermophoretic force to increase in case of incomplete NEAC and to decrease in case of incomplete TMAC. Moreover, this model leads the drag force to decrease as the accommodation coefficients decrease.

In the present work, the influence of the gas-surface interaction law on the drag and thermophoretic forces acting on a sphere of high thermal conductivity immersed in a monatomic rarefied gas is investigated by employing the Cercignani-Lampis model of gas-surface interaction. The kinetic equation proposed by Shakhov (1968) is solved numerically via a discrete velocity method which takes into account the discontinuity of the distribution function of molecular velocities around a convex body, see e.g. Sone (1966); Sone & Takata (1992). The viscous drag and the thermophoretic forces on the sphere, as well as the macroscopic characteristics of the gas flow around it, are calculated in a wide range of the gas rarefaction so that the free molecular, transition and hydrodynamic regimes are covered. The values of the TMAC and NEAC are chosen with basis on experimental data as given by Trott *et al.* (2011); Sharipov & Moldover (2016). The reciprocity relation between the cross phenomena is obtained and applied as an accuracy criterion for the numerical calculations. The results obtained for both the drag and thermophoretic forces on the sphere in the whole range of the gas rarefaction are compared to those results provided by Beresnev & Chernyak (1995); Beresnev *et al.* (1990); Takata & Sone (1992); Takata *et al.* (1993) in case of diffuse scattering on the surface. Moreover, the results obtained for the forces in the free molecular regime are compared to those presented by Chernyak & Sograbi (2019) in a wide range of TMAC and NEAC.

Regarding the comparison with experimental data, it is worth mentioning that although many data are available in the literature, such a comparison is still a difficult task because in most of the experiments the carrier gas is air or a polyatomic gas, and the results are limited to a certain range of the Knudsen number which usually covers the continuum and near-continuum regimes. Moreover, the experiments involve particles of different materials and some physical properties of matter, such as the thermal conductivity, may play an important role in the description of phoretic phenomena. A list of measurements concerning thermophoresis on spherical particles can be found in the review by Young (2011), while a critical review on the drag force on a sphere in the transition regime which includes experimental data is given by Bailey *et al.* (2004). In the present work, a comparison with the more recent data on thermophoresis provided by Bosworth *et al.* (2016) in case of a copper sphere in argon gas is presented.

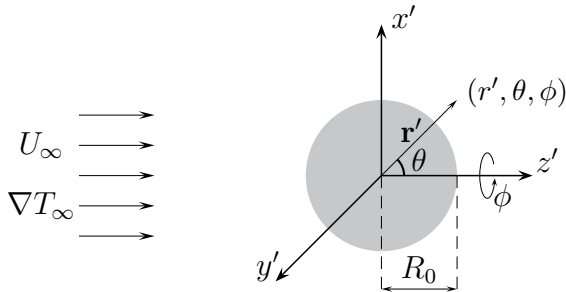


FIGURE 1. Formulation of the problem

2. Formulation of the problem

It is considered a sphere of radius R_0 at rest placed in a monoatomic rarefied gas. Far from the sphere, the gas flows with a constant bulk velocity U_∞ and has a temperature gradient $\nabla T_\infty = \partial T / \partial z'$ in the z' -direction as shown in figure 1. Due to the problem geometry, it is convenient to introduce spherical coordinates (r', θ, ϕ) in the physical space. Then, according to figure 1, the components of the position vector \mathbf{r}' of gas molecules are given as

$$x' = r' \sin \theta \cos \phi, \quad (2.1a)$$

$$y' = r' \sin \theta \sin \phi, \quad (2.1b)$$

$$z' = r' \cos \theta. \quad (2.1c)$$

Moreover, the components of the molecular velocity vector \mathbf{v} read

$$v_x = (v_r \sin \theta + v_\theta \cos \theta) \cos \phi - v_\phi \sin \phi, \quad (2.2a)$$

$$v_y = (v_r \sin \theta + v_\theta \cos \theta) \sin \phi + v_\phi \cos \phi, \quad (2.2b)$$

$$v_z = v_r \cos \theta - v_\theta \sin \theta, \quad (2.2c)$$

where v_r , v_θ and v_ϕ are the radial, polar and azimuthal components of the molecular velocity vector, respectively, which are written in spherical coordinates (v, θ', ϕ') in the velocity space as follows

$$v_r = v \cos \theta', \quad (2.3a)$$

$$v_\theta = v \sin \theta' \cos \phi', \quad (2.3b)$$

$$v_\phi = v \sin \theta' \sin \phi', \quad (2.3c)$$

with the tangential component given as

$$v_t = \sqrt{v_\theta^2 + v_\phi^2} = v \sin \theta'. \quad (2.4)$$

It is assumed that the thermal conductivity of the spherical particle is significantly higher than that corresponding to the carrier gas. As a consequence, the temperature of the sphere is uniform and equal to the gas temperature in equilibrium far from the sphere. Let us denote by n_0 , T_0 and p_0 the number density, temperature and pressure of the gas in thermodynamic equilibrium, respectively. Two dimensionless thermodynamic forces are introduced here as follows

$$X_u = \frac{U_\infty}{v_0}, \quad X_T = \frac{\ell_0}{T_0} \frac{\partial T}{\partial z'}, \quad (2.5)$$

where ℓ_0 and v_0 denote the equivalent free path and the most probable molecular velocity,

defined as

$$v_0 = \sqrt{\frac{2kT_0}{m}}, \quad \ell_0 = \frac{\mu_0 v_0}{p_0}. \quad (2.6)$$

μ_0 denotes the viscosity of the gas at temperature T_0 , while m and k are the molecular mass and the Boltzmann constant. It is assumed the smallness of the thermodynamic forces defined in (2.5), i.e.

$$|X_u| \ll 1, \quad |X_T| \ll 1. \quad (2.7)$$

These assumptions of weak disturbance from equilibrium allow us to split the problem into two independent parts corresponding to viscous drag and thermophoresis on the sphere. Hereafter, the dimensionless radius and also the position and molecular velocity vectors are introduced as follows

$$r_0 = \frac{R_0}{\ell_0}, \quad \mathbf{r} = \frac{\mathbf{r}'}{\ell_0}, \quad \mathbf{c} = \frac{\mathbf{v}}{v_0}. \quad (2.8)$$

The pressure of the gas is constant and given by the state equation of an ideal gas as $p_0 = n_0 k T_0$. As a consequence, the asymptotic behavior of the number density $n(\mathbf{r})$ and temperature $T(\mathbf{r})$ of the gas far from the sphere are given as

$$n_\infty = \lim_{r \rightarrow \infty} n(\mathbf{r}) = n_0(1 - zX_T), \quad (2.9a)$$

$$T_\infty = \lim_{r \rightarrow \infty} T(\mathbf{r}) = T_0(1 + zX_T). \quad (2.9b)$$

The main parameter of the problem is the rarefaction parameter, δ , which is inversely proportional to the Knudsen number, but defined as the ratio of the sphere radius to the equivalent molecular free path, i.e.

$$\delta = \frac{R_0}{\ell_0} = r_0. \quad (2.10)$$

When $\delta \ll 1$ the gas is in the free molecular regime, while the opposite limit, $\delta \gg 1$, corresponds to the continuum or hydrodynamic regime. In other situations, the gas is in the so called transition regime.

The model of gas-surface interaction law proposed by Cercignani & Lampis (1971) is employed in the boundary condition. According to this model, the type of the gas-surface interaction is chosen by setting appropriate values of NEAC and TMAC. Henceforth, these accommodation coefficients will be denoted by α_n and α_t , respectively. The diffuse scattering or complete accommodation on the surface corresponds to $\alpha_n=1$ and $\alpha_t=1$.

The viscous drag and thermophoretic forces acting on the sphere are calculated in a wide range of the gas rarefaction parameter, δ , so that all the regimes of the gas flow are covered. Moreover, various values of accommodation coefficients are considered in the calculations in order to analyse the influence of the gas-surface interaction law on the solution of the problem. The flow fields, i.e. the profiles of the density and temperature deviations from equilibrium, bulk velocity and heat flux, as functions of the radial distance from the sphere are also obtained. Some numerical results are compared to those found in the literature. The reciprocity relation between cross phenomena is obtained at arbitrary distance from the sphere and then verified numerically.

3. Kinetic equation

The problem is solved on the basis of the Boltzmann equation for arbitrary values of rarefaction parameter δ so that the free molecular, transition and continuum regimes are

covered. For the problem in question, the Boltzmann equation in the absence of external forces reads

$$\mathbf{v} \cdot \frac{\partial f}{\partial \mathbf{r}'} = Q(ff_*), \quad (3.1)$$

where $f=f(\mathbf{r}', \mathbf{v})$ is the distribution function of molecular velocities and $Q(ff_*)$ is the collision integral whose expression can be found in the literature, see e.g. Ferziger & Kaper (1972); Cercignani (1975); Kogan (1988). Here, the model proposed by Shakhov (1968) for the collision integral is employed due to its reliability to deal with problems regarding both mass and heat transfer. Then, the collision integral reads

$$Q(ff_*) = Q_S = \nu_S \left\{ f^M \left[1 + \frac{4}{15} \left(\frac{V^2}{v_0^2} - \frac{5}{2} \right) \frac{\mathbf{Q} \cdot \mathbf{V}}{p_0 v_0^2} \right] - f(\mathbf{r}', \mathbf{v}) \right\} \quad (3.2)$$

where f^M is the local Maxwellian function, $\mathbf{U}(\mathbf{r}')$ and $\mathbf{Q}(\mathbf{r}')$ are the bulk velocity and heat flux vectors. The quantity ν_S has the order of the intermolecular interaction frequency and $\mathbf{V}=\mathbf{v} - \mathbf{U}$ is the so called peculiar velocity.

The assumptions of smallness of the thermodynamic forces, given in (2.7), allow us to linearize the kinetic equation by representing the distribution function as follows

$$f(\mathbf{r}, \mathbf{c}) = f_R^M [1 + h^{(T)}(\mathbf{r}, \mathbf{v}) X_T + h^{(u)}(\mathbf{r}, \mathbf{v}) X_u], \quad (3.3)$$

where $h^{(T)}$ and $h^{(u)}$ are the perturbation functions due to the thermodynamic forces X_T and X_u . The reference Maxwellian function is given by

$$f_R^M = f^M = f_0 \left[1 + z \left(c^2 - \frac{5}{2} \right) X_T + 2c_z X_u \right], \quad (3.4)$$

where f_0 is the global Maxwellian function.

Then, after introducing the representation (3.3) into (3.1), and also introducing the dimensionless quantities given by (2.8), the linearized kinetic equation corresponding to each thermodynamic force is written as

$$\hat{D}h^{(n)} = \hat{L}_S h^{(n)} + g^{(n)}(\mathbf{r}, \mathbf{c}), \quad n = T, u, \quad (3.5)$$

where the operator

$$\hat{D} = \mathbf{c} \cdot \frac{\partial}{\partial \mathbf{r}} \quad (3.6)$$

and the linearized collision integral reads

$$\hat{L}_S h^{(n)} = \nu^{(n)} + \left(c^2 - \frac{5}{2} \right) \tau^{(n)} + 2\mathbf{c} \cdot \mathbf{u}^{(n)} + \frac{4}{15} \left(c^2 - \frac{5}{2} \right) \mathbf{c} \cdot \mathbf{q}^{(n)} - h^{(n)}. \quad (3.7)$$

The free terms are given by

$$g^{(T)} = -c_z \left(c^2 - \frac{5}{2} \right) \quad g^{(u)} = 0. \quad (3.8)$$

The dimensionless quantities in the right hand side of (3.7) correspond to the density and temperature deviations from equilibrium, bulk velocity and heat flux vectors, respectively, due to the corresponding thermodynamic force. These quantities are calculated in terms of the distribution function of molecular velocities, and details regarding these calculations are given by Ferziger & Kaper (1972). In our notation, these quantities are written in terms of the perturbation function $h^{(n)}$ corresponding to each thermodynamic force as

$$\nu^{(n)}(\mathbf{r}) = \frac{1}{\pi^{3/2}} \int h^{(n)}(\mathbf{r}, \mathbf{c}) e^{-c^2} d\mathbf{c}, \quad (3.9)$$

$$\tau^{(n)}(\mathbf{r}) = \frac{2}{3\pi^{3/2}} \int \left(c^2 - \frac{3}{2} \right) h^{(n)}(\mathbf{r}, \mathbf{c}) e^{-c^2} d\mathbf{c}, \quad (3.10)$$

$$\mathbf{u}^{(n)}(\mathbf{r}) = \frac{1}{\pi^{3/2}} \int \mathbf{c} h^{(n)}(\mathbf{r}, \mathbf{c}) e^{-c^2} d\mathbf{c}, \quad (3.11)$$

$$\mathbf{q}^{(n)}(\mathbf{r}) = \frac{1}{\pi^{3/2}} \int \mathbf{c} \left(c^2 - \frac{5}{2} \right) h^{(n)}(\mathbf{r}, \mathbf{c}) e^{-c^2} d\mathbf{c}. \quad (3.12)$$

Far from the sphere, i.e. in the limit $\mathbf{r} \rightarrow \infty$, the asymptotic behavior of the perturbation functions are obtained from the Chapmann-Enskog solution for the linearized kinetic equation as

$$h_{\infty}^{(T)} = \lim_{\mathbf{r} \rightarrow \infty} h^{(T)}(\mathbf{r}, \mathbf{c}) = -\frac{3}{2} c_z \left(c^2 - \frac{5}{2} \right), \quad (3.13)$$

$$h_{\infty}^{(u)} = \lim_{\mathbf{r} \rightarrow \infty} h^{(u)}(\mathbf{r}, \mathbf{c}) = 0. \quad (3.14)$$

Due to the spherical geometry of the problem, it is convenient to write the kinetic equation (3.5) in spherical coordinates in both physical and molecular velocity spaces. Details regarding this transformation are given by Shakhov (1967). Moreover, the problem has symmetry on the azimuthal angle ϕ . Therefore, after some algebraic manipulation, the left hand side of the kinetic equation (3.5) is written as follows

$$\hat{D}h^{(n)} = c_r \frac{\partial h^{(n)}}{\partial r} - \frac{c_t}{r} \frac{\partial h^{(n)}}{\partial \theta'} + \frac{c_t}{r} \cos \phi' \frac{\partial h^{(n)}}{\partial \theta} - \frac{c_t}{r} \sin \phi' \cot \theta \frac{\partial h^{(n)}}{\partial \phi'} \quad (3.15)$$

where $h^{(n)} = h^{(n)}(r, \theta, \mathbf{c})$ and $\mathbf{c} = (c, \theta', \phi')$. The symmetry of the solution on the azimuthal angle also allows us to eliminate the dependence of the moments of the perturbation function which appear in the right hand side of the kinetic equation on the angle ϕ . Thus, the density and temperature deviations given in (3.9) and (3.10) are written as

$$\nu^{(n)}(r, \theta) = \frac{1}{\pi^{3/2}} \int h^{(n)}(r, \theta, \mathbf{c}) e^{-c^2} d\mathbf{c} \quad (3.16)$$

$$\tau^{(n)}(r, \theta) = \frac{2}{3\pi^{3/2}} \int \left(c^2 - \frac{3}{2} \right) h^{(n)}(r, \theta, \mathbf{c}) e^{-c^2} d\mathbf{c}, \quad (3.17)$$

where $d\mathbf{c} = c^2 \sin \theta' dc d\theta' d\phi'$. Moreover, the nonzero components of the bulk velocity and heat flux vectors given in (3.11) and (3.12) are written as

$$u_r^{(n)}(r, \theta) = \frac{1}{\pi^{3/2}} \int c_r h^{(n)}(r, \theta, \mathbf{c}) e^{-c^2} d\mathbf{c}, \quad (3.18)$$

$$u_{\theta}^{(n)}(r, \theta) = \frac{1}{\pi^{3/2}} \int c_{\theta} h^{(n)}(r, \theta, \mathbf{c}) e^{-c^2} d\mathbf{c}, \quad (3.19)$$

$$q_r^{(n)}(r, \theta) = \frac{1}{\pi^{3/2}} \int c_r \left(c^2 - \frac{5}{2} \right) h^{(n)}(r, \theta, \mathbf{c}) e^{-c^2} d\mathbf{c}, \quad (3.20)$$

$$q_{\theta}^{(n)}(r, \theta) = \frac{1}{\pi^{3/2}} \int c_{\theta} \left(c^2 - \frac{5}{2} \right) h^{(n)}(r, \theta, \mathbf{c}) e^{-c^2} d\mathbf{c}. \quad (3.21)$$

Similarly to the moments appearing in the kinetic equation, the force on the sphere in

the z' -direction is calculated in terms of the distribution function of molecular velocities as follows

$$F'_z = - \int_{\Sigma'_w} d\Sigma'_w \int m v_r v_z f(\mathbf{r}, \mathbf{v}) d\mathbf{v} \quad (3.22)$$

where $d\Sigma'_w = R_0^2 \sin \theta d\theta d\phi$ is an area element taken in the surface of the sphere. For convenience, the dimensionless force is introduced here as

$$F_z = \frac{F'_z}{4\pi R_0^2 p_0}. \quad (3.23)$$

Then, after the introduction of the representation (3.3) into (3.22) and some algebraic manipulation, the dimensionless force acting on the sphere reads

$$F_z = F_T X_T + F_u X_u, \quad (3.24)$$

where the dimensionless thermophoretic and drag forces are given as

$$F_T = -\frac{1}{2\pi^{5/2}} \int_{\Sigma_w} d\Sigma_w \int c_r c_z e^{-c^2} \left[h^{(T)} + z_0 \left(c^2 - \frac{5}{2} \right) \right] d\mathbf{c}, \quad (3.25)$$

$$F_u = -\frac{1}{2\pi^{5/2}} \int_{\Sigma_w} d\Sigma_w \int c_r c_z e^{-c^2} (h^{(u)} + 2c_z) d\mathbf{c}, \quad (3.26)$$

with $d\Sigma_w = d\Sigma'_w / R_0^2$.

4. Boundary condition

The boundary conditions for both the drag and the thermophoresis on the sphere are obtained from the relation between the distribution functions of incident particles on the wall and reflected particles from the wall. According to Cercignani (1975); Sharipov (2016), the general form of the linearized boundary condition at the surface reads

$$h^{+(n)} = \hat{A} h^{-(n)} + h_w^{(n)} - \hat{A} h_w^{(n)}, \quad (4.1)$$

where the signal $+$ denotes the reflected particles from the surface, while the signal $-$ denotes the incident particles on the surface. From (3.4), the source terms are given as

$$h_w^{(u)} = -2c_z, \quad h_w^{(T)} = -z_0 \left(c^2 - \frac{5}{2} \right), \quad (4.2)$$

where $z_0 = r_0 \cos \theta$ and $c_z = c_r \cos \theta - c_\theta \sin \theta$.

For the problem in question, the scattering operator \hat{A} is expressed as

$$\hat{A} h^{(n)} = \hat{A}_r \hat{A}_\theta \hat{A}_\phi h^{(n)}, \quad (4.3)$$

where

$$\hat{A}_r \xi = -\frac{1}{c_r} \int_{c'_r < 0} c'_r \exp(c_r^2 - c'^2_r) R_r(c_r \rightarrow c'_r) \xi dc'_r, \quad (4.4)$$

$$\hat{A}_i \xi = \int_{-\infty}^{\infty} \exp(c_i^2 - c'^2_i) R_i(c_i \rightarrow c'_i) \xi dc'_i, \quad i = \theta, \phi, \quad (4.5)$$

for an arbitrary ξ as function of the molecular velocity. The scattering kernel proposed by Cercignani and Lampis is decomposed as follows

$$R(\mathbf{c} \rightarrow \mathbf{c}') = R_r(c_r \rightarrow c'_r) R_\theta(c_\theta \rightarrow c'_\theta) R_\phi(c_\phi \rightarrow c'_\phi), \quad (4.6)$$

where

$$R_r(c_r \rightarrow c'_r) = \frac{2c_r}{\alpha_n} \exp \left[-\frac{c_r^2 + (1 - \alpha_n)c_r'^2}{\alpha_n} \right] I_0 \left(\frac{2\sqrt{1 - \alpha_n}}{\alpha_n} c_r c'_r \right), \quad (4.7)$$

$$R_i(c_i \rightarrow c'_i) = \frac{1}{\sqrt{\pi\alpha_t(2 - \alpha_t)}} \exp \left\{ -\frac{[c_i - (1 - \alpha_t)c'_i]^2}{\alpha_t(2 - \alpha_t)} \right\}, \quad i = \theta, \phi. \quad (4.8)$$

I_0 denotes the modified Bessel function of first kind and zeroth order given by Abramowitz & Stegun (1972). According to this model, the accommodation coefficients can vary in the ranges $0 \leq \alpha_t \leq 2$ and $0 \leq \alpha_n \leq 1$. The case $\alpha_t=1$ and $\alpha_n=1$ corresponds to diffuse scattering or complete accommodation on the spherical surface, while the case $\alpha_t=0$ and $\alpha_n=0$ corresponds to specular reflection at the surface. It is worth noting that, for intermediate values of α_t and α_n the scattering kernel proposed by Cercignani-Lampis differs significantly from the diffuse-specular model proposed by Maxwell, in which just one accommodation coefficient was introduced.

It can be shown that the following relations are satisfied

$$\hat{A}_i c_i = (1 - \alpha_t) c_i, \quad i = \theta, \phi, \quad (4.9)$$

$$\hat{A}_i c_i^2 = (1 - \alpha_t)^2 c_i^2 + \frac{1}{2} \alpha_t (2 - \alpha_t), \quad (4.10)$$

$$\hat{A}_i c_i^3 = (1 - \alpha_t)^3 c_i^3 + \frac{3}{2} \alpha_t (2 - \alpha_t) (1 - \alpha_t) c_i, \quad (4.11)$$

$$\hat{A}_r c_r = -\sqrt{\alpha_n} H_1(\eta), \quad (4.12)$$

$$\hat{A}_r c_r^2 = \alpha_n + (1 - \alpha_n) c_r^2, \quad (4.13)$$

$$\hat{A}_r c_r^3 = -\alpha_n^{3/2} H_3(\eta), \quad (4.14)$$

where

$$H_j(\eta) = 2e^{-\eta^2} \int_0^\infty \xi^{j+1} e^{-\xi^2} I_0(2\eta\xi) d\xi, \quad \xi = \frac{c'_r}{\sqrt{\alpha_n}}, \quad j = 1, 3, \quad (4.15)$$

and

$$\eta = c_r \sqrt{\frac{1}{\alpha_n} - 1}. \quad (4.16)$$

Therefore, with the help of the relations (4.9)-(4.14), the boundary conditions at $r=r_0$ and $c_r > 0$, for each thermodynamic force are obtained from (4.1) as

$$h^{+(T)} = \hat{A} h^{-(T)} + z_0 [\alpha_n (1 - c_r^2) + \alpha_t (2 - \alpha_t) (1 - c_t^2)], \quad (4.17)$$

$$h^{+(u)} = \hat{A} h^{-(u)} - 2 \frac{z_0}{\delta} [(1 - \alpha_t) c_r + \sqrt{\alpha_n} H_1(\eta)] - 2 \alpha_t c_z. \quad (4.18)$$

5. Reciprocity relation

As it is known from the non-equilibrium thermodynamics, see e.g. De Groot & Mazur (1984), the reciprocity relations between cross phenomena represent an important criterion to verify the numerical precision in calculations regarding small deviations from

thermodynamic equilibrium. According to Sharipov (2006); Sharipov & Kalempa (2006); Sharipov (2010), the reciprocity relation for the problem in question can be written as

$$A_{uT}^t = A_{Tu}^t, \quad (5.1)$$

where the time-reversal kinetic coefficients are defined as

$$A_{kn}^t = ((\hat{T}g^{(k)}, h^{(n)})) + \int_{\Sigma_w} (\hat{T}v_r h_w^{(k)}, h^{(n)}) d\Sigma + \frac{1}{2} \int_{\Sigma_g} (\hat{T}v_r h^{(k)}, h^{(n)}) d\Sigma. \quad (5.2)$$

The dimension free terms $g^{(n)} = v_0 g^{(n)} / \ell_0$ ($n = u, T$), where $g^{(n)}$ are given in (3.8). The source terms $h_w^{(n)}$ are given in (4.2). Here, the time reversal operator \hat{T} just changes the sign of the molecular velocity, i.e. $\hat{T}h(\mathbf{v}) = h(-\mathbf{v})$. The scalar products are defined as

$$(\xi_1, \xi_2) = \int f_0 \xi_1(\mathbf{r}', \mathbf{v}) \xi_2(\mathbf{r}', \mathbf{v}) d\mathbf{v}, \quad (5.3)$$

and

$$((g, h)) = \int_{\Omega} (g, h) d\mathbf{r}'. \quad (5.4)$$

Ω means the gas flow domain, while Σ_w and Σ_g mean the solid spherical surface and the imaginary spherical surface at $r' \rightarrow \infty$ which enclose the gas domain.

Then, after some algebraic manipulation, the time reversed kinetic coefficients are written as

$$A_{uT}^t = -4\pi R_0^2 n_0 v_0 F_T - \frac{1}{2} \int_{\Sigma_g} (\hat{T}v_r h^{(T)}, h^{(u)}) d\Sigma, \quad (5.5)$$

$$A_{Tu}^t = v_0 n_0 \int_{\Sigma_g} z q_r^{(u)}(r, \theta) d\Sigma + \frac{1}{2} \int_{\Sigma_g} (\hat{T}v_r h^{(T)}, h^{(u)}) d\Sigma. \quad (5.6)$$

Therefore, after substituting (5.5) and (5.6) into (5.1), the thermophoretic force on the sphere is related to the solution of the drag force problem as

$$F_T = -\frac{r^2}{2\delta^2} \left[r \int_0^\pi q_r^{(u)}(r, \theta) \cos \theta \sin \theta d\theta + \frac{1}{\pi^{3/2}} \int_0^\pi \int c_r h^{(T)}(r, \theta, -\mathbf{c}) h^{(u)}(r, \theta, \mathbf{c}) e^{-c^2} \sin \theta d\mathbf{c} d\theta \right], \quad (5.7)$$

where r is the radius of the imaginary spherical surface Σ_g , which can be arbitrary. The right hand side of the relation (5.7) was calculated numerically for $r=0, 5, 10$ and 40 and the fulfillment of such a relation was verified numerically within the numerical error of 0.1% .

6. Method of solution

6.1. Free molecular regime

In the free molecular regime, i.e. $\delta \ll 1$, the collision integral which appears in the Boltzmann equation (3.1) can be neglected. As a consequence, in this regime of the gas flow, the problem is solved analytically via solution of a differential equation for each thermodynamic force obtained from (3.5) as

$$\hat{D}h^{(n)} = g^{(n)}, \quad (6.1)$$

whose solutions must satisfy the boundary conditions given in (4.1). Moreover, in this regime of the gas flow, the distribution function of incident gas particles on the surface is

not perturbed, which means that $h^{-(n)} = h_\infty^{(n)}$ as given by (3.13) and (3.14). The method of the characteristics allows us to solve the previous equations for each thermodynamic force and, thus, obtain the following solutions

$$h^{(n)}(r, \theta, \mathbf{c}) = \begin{cases} h_c^{(n)} \cos \theta + h_s^{(n)} c_\theta \sin \theta + g^{(n)} \frac{S}{c}, & 0 \leq \theta' \leq \theta_0, \\ h_\infty^{(n)}, & \theta_0 \leq \theta' \leq \pi, \end{cases} \quad (6.2)$$

where

$$h_c^{(n)}(r, c, \theta') = C_1^{(n)} \left(r - \frac{S}{c} c_r \right) - C_2^{(n)} c_r, \quad (6.3)$$

$$h_s^{(n)}(r, c, \theta') = C_1^{(n)} \frac{S}{c} + C_2^{(n)}. \quad (6.4)$$

S is the distance between a point in the gas flow domain with Cartesian coordinates (x, y, z) and a point in the spherical surface with Cartesian coordinates (x_0, y_0, z_0) which is written as

$$S = r \cos \theta' - \sqrt{r_0^2 - r^2 \sin^2 \theta'}. \quad (6.5)$$

It is worth noting that the vector \mathbf{S} is directed towards $-\mathbf{c}$ and, consequently, the following relation is valid

$$z_0 = z - \frac{S}{c} c_z. \quad (6.6)$$

The angle θ_0 is given by

$$\theta_0 = \arcsin \left(\frac{r_0}{r} \right). \quad (6.7)$$

The quantities $C_1^{(n)}$ and $C_2^{(n)}$ are obtained from the boundary conditions given in (4.17) and (4.18) as

$$C_1^{(T)} = -\frac{3}{2r_0} \left\{ \alpha_n^{3/2} H_3(\eta) + \alpha_n^{1/2} H_1(\eta) \left[\alpha_t(2 - \alpha_t) + (1 - \alpha_t)^2 c_t^2 - \frac{5}{2} \right] \right\} \\ + \alpha_n(1 - c_r^2) + \alpha_t(2 - \alpha_t) - \alpha_t(2 - \alpha_t) c_t^2 + \frac{2\alpha_t c_r}{r_0} \quad (6.8)$$

$$C_2^{(T)} = \frac{3}{2}(1 - \alpha_t) \left[\alpha_n + (1 - \alpha_n) c_r^2 + (1 - \alpha_t)^2 c_t^2 + 2\alpha_t(2 - \alpha_t) - \frac{5}{2} \right]. \quad (6.9)$$

$$C_1^{(u)} = -\frac{2[(1 - \alpha_t) c_r + \sqrt{\alpha_n} H_1(\eta)]}{r_0}, \quad (6.10)$$

$$C_2^{(u)} = 2\alpha_t, \quad (6.11)$$

where $H_1(\eta)$ and $H_3(\eta)$ are defined in (4.15).

Then, the thermophoretic and drag forces on the sphere are obtained from (3.25) and (3.26) as

$$F_T = -\frac{1}{2\sqrt{\pi}} \left(\frac{1 + \alpha_t}{2} + \mathcal{H} \right), \quad (6.12)$$

$$F_u = \frac{2}{3\sqrt{\pi}} \left(1 + \alpha_t + 2\alpha_n^{1/2} \int_0^\infty c_r^2 e^{-c_r^2} H_1(\eta) \, dc_r \right), \quad (6.13)$$

where

$$\mathcal{H} = \alpha_n^{1/2} \int_0^\infty c_r^2 e^{-c_r^2} \left[\alpha_n H_3(\eta) - \frac{3}{2} H_1(\eta) \right] dc_r, \quad (6.14)$$

with η and ξ defined in (4.15) and (4.16), respectively.

In case of diffuse scattering, i.e. $\alpha_t=1$ and $\alpha_n=1$, the thermophoretic and drag forces given in (6.12) and (6.13) correspond to those found in the literature, see e.g. Takata *et al.* (1993); Beresnev & Chernyak (1995); Sone (2007).

The macroscopic characteristics of the gas flow around the sphere due to each thermodynamic force can be obtained just by substituting the corresponding solution given in (6.2) into the expressions (3.16)-(3.21).

6.2. Arbitrary gas rarefaction

In order to consider arbitrary values of the gas rarefaction, the problem is solved numerically by employing the linearized kinetic equations given in (3.15) for each thermodynamic force subject to the corresponding boundary condition. Here, these equations are solved by the discrete velocity method, whose details can be found in the literature, see e.g. Sharipov & Subbotin (1993); Sharipov (2016). Moreover, the split method proposed by Naris & Valougeorgis (2005) to deal with the problem of the discontinuity of the distribution function of molecular velocities is employed. In rarefied gas dynamics, the problem of the discontinuity of the distribution function is a peculiarity inherent to gas flows around convex bodies, see e.g. Sone & Takata (1992), and must be treated carefully when a finite difference scheme is used. The idea of the split method is the decomposition of the perturbation function into two parts as

$$h^{(n)}(\mathbf{r}, \mathbf{c}) = h_0^{(n)}(\mathbf{r}, \mathbf{c}) + \tilde{h}^{(n)}(\mathbf{r}, \mathbf{c}), \quad (6.15)$$

where the function $h_0^{(n)}$ is obtained from the solution of the differential equation

$$\hat{D}h_0^{(n)} - h_0^{(n)} = 0, \quad (6.16)$$

with boundary conditions

$$h_0^{+(n)} = \hat{A}h_\infty^{(n)} + h_w^{(n)} - \hat{A}h_w^{(n)}, \quad (6.17)$$

where $h_w^{(n)}$ and $h_\infty^{(n)}$ are given in (4.2), (3.13) and (3.14). Note that, the discontinuous perturbation function $h_0^{(n)}$ can be obtained analytically by the characteristics method. Thus, the solution of equation (6.16) subject to the boundary condition (6.17), is written as follows

$$h_0^{(n)}(r, \theta, \mathbf{c}) = \begin{cases} [h_c^{(n)} \cos \theta + h_s^{(n)} c_\theta \sin \theta] e^{-S/c}, & 0 \leq \theta' \leq \theta_0, \\ h_\infty^{(n)}, & \theta_0 < \theta' \leq \pi, \end{cases} \quad (6.18)$$

where the distance S along the characteristic line and the angle θ_0 are given in (6.5) and (6.7), while the functions $h_c^{(n)}$ and $h_s^{(n)}$ correspond to those given in (6.3) and (6.4) in the free molecular regime. Note that the moments (3.16)-(3.21) are also decomposed into two parts as

$$\Lambda^{(n)} = \Lambda_0^{(n)} + \tilde{\Lambda}^{(n)}, \quad \Lambda^{(n)} = \nu^{(n)}, \tau^{(n)}, u_r^{(n)}, q_r^{(n)}, u_\theta^{(n)}, q_\theta^{(n)}, \quad (6.19)$$

where the quantities with tilde are calculated by the same expressions given in (3.16)-(3.21), just replacing $h^{(n)}$ by $\tilde{h}^{(n)}$, while the quantities with zero index are calculated in terms of the known solutions $h_0^{(n)}$ given in (6.18).

The function $\tilde{h}^{(n)}$ satisfy the kinetic equation (3.5) just replacing $h^{(n)}$ by $\tilde{h}^{(n)}$, but with the boundary condition

$$\tilde{h}^{+(n)} = \hat{A}\tilde{h}^{-(n)}. \quad (6.20)$$

The advantage of the split method is that the function $\tilde{h}^{(n)}$ is sufficiently smooth so that a finite difference scheme leads to a smaller numerical error. To reduce the number of variables of the perturbation function $\tilde{h}^{(n)}$, its dependence on the variables θ and ϕ' is eliminated by employing the similarity solution proposed by Sone & Aoki (1983). Then, in our notation, the perturbation function $\tilde{h}^{(n)}$ is represented as

$$\tilde{h}^{(n)}(r, \theta, \mathbf{c}) = \Phi^{(n)}(r, c, \theta') \cos \theta + \Psi^{(n)}(r, c, \theta') c_\theta \sin \theta. \quad (6.21)$$

Then, the substitution of the representation (6.21) into the kinetic equation (3.5) allows us to obtain a system of equations for the new perturbation functions $\Phi^{(n)}$ and $\Psi^{(n)}$ corresponding to each thermodynamic force given as

$$\begin{aligned} c_r \frac{\partial \Phi^{(n)}}{\partial r} - \frac{c_t}{r} \frac{\partial \Phi^{(n)}}{\partial \theta'} + \frac{c_t^2}{r} \Psi^{(n)} &= \nu^{*(n)} + \left(c^2 - \frac{3}{2}\right) \tau^{*(n)} + 2c_r u_r^{*(n)} \\ &+ \frac{4}{15} c_r \left(c^2 - \frac{5}{2}\right) q_r^{*(n)} - \Phi^{(n)} + g_1^{*(n)}, \end{aligned} \quad (6.22)$$

$$\begin{aligned} c_r \frac{\partial \Psi^{(n)}}{\partial r} - \frac{c_t}{r} \frac{\partial \Psi^{(n)}}{\partial \theta'} - \frac{c_r}{r} \Psi^{(n)} - \frac{1}{r} \Phi^{(n)} &= 2u_\theta^{*(n)} \\ &+ \frac{4}{15} \left(c^2 - \frac{5}{2}\right) q_\theta^{*(n)} - \Psi^{(n)} + g_2^{*(n)}, \end{aligned} \quad (6.23)$$

where the free terms read

$$g_1^{*(T)} = -c_r \left(c^2 - \frac{5}{2}\right), \quad g_2^{*(T)} = c^2 - \frac{5}{2}, \quad g_1^{*(u)} = g_2^{*(u)} = 0. \quad (6.24)$$

The dimensionless moments which appear in the right hand side of equations (6.22) and (6.23) are obtained from (3.16)-(3.21) as

$$\nu^{*(n)}(r) = \frac{\nu_0^{(n)}(r)}{\cos \theta} + \frac{2}{\sqrt{\pi}} \int_0^\infty \int_0^\pi c_t \Phi^{(n)} e^{-c^2} c d c d \theta', \quad (6.25)$$

$$\tau^{*(n)}(r) = \frac{\tau_0^{(n)}(r)}{\cos \theta} + \frac{4}{3\sqrt{\pi}} \int_0^\infty \int_0^\pi \left(c^2 - \frac{3}{2}\right) c_t \Phi^{(n)} e^{-c^2} c d c d \theta', \quad (6.26)$$

$$u_r^{*(n)}(r) = \frac{u_{r0}^{(n)}(r)}{\cos \theta} + \frac{2}{\sqrt{\pi}} \int_0^\infty \int_0^\pi c_r c_t \Phi^{(n)} e^{-c^2} c d c d \theta', \quad (6.27)$$

$$u_\theta^{*(n)}(r) = \frac{u_{\theta 0}^{(n)}(r)}{\sin \theta} + \frac{1}{\sqrt{\pi}} \int_0^\infty \int_0^\pi c_t^3 \Psi^{(n)} e^{-c^2} c d c d \theta', \quad (6.28)$$

$$q_r^{*(n)}(r) = \frac{q_{r0}^{(n)}(r)}{\cos \theta} + \frac{2}{\sqrt{\pi}} \int_0^\infty \int_0^\pi c_r c_t \left(c^2 - \frac{5}{2}\right) \Phi^{(n)} e^{-c^2} c d c d \theta', \quad (6.29)$$

$$q_\theta^{*(n)}(r) = \frac{q_{\theta 0}^{(n)}(r)}{\sin \theta} + \frac{1}{\sqrt{\pi}} \int_0^\infty \int_0^\pi c_t^3 \left(c^2 - \frac{5}{2}\right) \Psi^{(n)} e^{-c^2} c d c d \theta'. \quad (6.30)$$

Far from the sphere the asymptotic behavior of the functions $\Phi^{(n)}$ and $\Psi^{(n)}$ are obtained from (3.13) and (3.14) as

$$\Phi_{\infty}^{(T)} = \lim_{r \rightarrow \infty} \Phi^{(T)} = -\frac{3}{2}c_r \left(c^2 - \frac{5}{2} \right), \quad \Psi_{\infty}^{(T)} = \lim_{r \rightarrow \infty} \Psi^{(T)} = \frac{3}{2} \left(c^2 - \frac{5}{2} \right), \quad (6.31)$$

$$\Phi_{\infty}^{(u)} = \lim_{r \rightarrow \infty} \Phi^{(u)} = 0, \quad \Psi_{\infty}^{(u)} = \lim_{r \rightarrow \infty} \Psi^{(u)} = 0. \quad (6.32)$$

The representation (6.21) allows us to write the dimensionless forces given in (3.25) and (3.26) as

$$\begin{aligned} F_n = & -\frac{4}{3\sqrt{\pi}} \int_{-\infty}^{\infty} \int_{-\infty}^{\infty} c_r^2 c_t \Phi^{(n)}(r_0, c_r, c_t) e^{-c^2} dc_r dc_t \\ & + \frac{4}{3\sqrt{\pi}} \int_{-\infty}^{\infty} \int_{-\infty}^{\infty} c_r c_t^3 \Psi^{(n)}(r_0, c_r, c_t) e^{-c^2} dc_r dc_t. \end{aligned} \quad (6.33)$$

Regarding the boundary conditions, the representation (6.21) is compatible with the Cercignani-Lampis boundary condition taking the following form

$$\hat{A}h^{-(n)} = \cos \theta \hat{A}_r \hat{A}_t^{(0)} \Phi^{-(n)} + c_t \cos \phi' \hat{A}_r \hat{A}_t^{(1)} \Psi^{-(n)}, \quad (6.34)$$

where

$$\begin{aligned} \hat{A}_r \xi = & \frac{2}{\alpha_n} \int_0^{\infty} c'_r \exp \left[-\frac{(1 - \alpha_n)c_r^2 + c_r'^2}{\alpha_n} \right] \\ & \times I_0 \left(\frac{2\sqrt{1 - \alpha_n}c_r c'_r}{\alpha_n} \right) \xi(-c'_r, c'_t) dc'_r, \end{aligned} \quad (6.35)$$

$$\begin{aligned} \hat{A}_t^{(i)} \xi = & \frac{2}{\alpha_t(2 - \alpha_t)} \int_0^{\infty} c'_t \exp \left[-\frac{(1 - \alpha_t)c_t^2 + c_t'^2}{\alpha_t(2 - \alpha_t)} \right] \\ & \times I_i \left[\frac{2(1 - \alpha_t)c_t c'_t}{\alpha_t(2 - \alpha_t)} \right] \xi(c'_r, c'_t) dc'_t, \end{aligned} \quad (6.36)$$

where I_i ($i=0, 1$) is the modified Bessel function of first kind and i -th order.

Therefore, the boundary conditions for the perturbation functions $\Phi^{(n)}$ and $\Psi^{(n)}$ are obtained from (4.17) and (4.18) as follows

$$\Phi^{+(n)} = \hat{A}_r \hat{A}_t^{(0)} \Phi^{-(n)}, \quad \Psi^{+(n)} = \hat{A}_r \hat{A}_t^{(1)} \Psi^{-(n)}. \quad (6.37)$$

Then, the system of kinetic equations (6.22) and (6.23) for each thermodynamic force, subject to the corresponding conditions (6.31)-(6.32) and (6.37), were solved numerically via the discrete velocity method with an accuracy of 0.1% for the moments of the perturbation functions. Such an accuracy was estimated by varying the grid parameters N_r , N_c and N_{θ} corresponding to the number of nodes in the radial coordinate r , molecular speed c and angle θ' . Moreover, the reciprocal relation 5.7 was verified.

7. Results and discussion

7.1. Free molecular regime

Firstly, the results obtained from the analytic solutions (6.12) and (6.13) were compared to those given by Chernyak & Sograbi (2019) in the free molecular regime. Figures (2) and (3) show the profiles of the dimensionless thermophoretic and drag forces on the sphere as functions of the TMAC, α_t , and fixed values of NEAC corresponding to $\alpha_n =$

0.1, 0.5 and 0.9. Figures (4) and (5) show the forces on the sphere as functions of the NEAC and fixed values of TMAC corresponding to $\alpha_t=0, 0.4, 0.8$ and 1. The analytic expressions given by Chernyak & Sograbi (2019) to calculate these forces were obtained in the limit $(1-\alpha_t) \ll 1$ and $(1-\alpha_n) \ll 1$, which means almost complete accommodation of gas particles on the sphere. According to figures (2) and (4), there is a good agreement between the results obtained in the present work and those given by Chernyak & Sograbi (2019) for the drag force in the whole range of accommodation coefficients. There is a small difference between the results only for small values of NEAC. On the contrary, as one can see from figures (3) and (5), there is a large disagreement between the present results and those given by Chernyak & Sograbi (2019) for the thermophoretic force in the whole range of accommodation coefficients. Note that, even in the limit of diffuse scattering such a disagreement is still large. However, it was verified numerically that the reciprocity relation given by (5.7) is fulfilled within an accuracy of 0.1% for arbitrary values of accommodation coefficients. Table 1 presents the comparison between the values of the thermophoretic force on the sphere calculated by (5.7) and (6.12). Moreover, numerical results for both forces in the free molecular regime are given in tables 2 and 3. As one can see from these tables, the numerical results obtained via kinetic equation for small value of rarefaction parameter tend to those given by (6.12) and (6.13). Therefore, since the reciprocity relation between cross phenomena was not verified by Chernyak & Sograbi (2019), the disagreement between the results for the thermophoretic force should be explained by some error in the derivation of the analytic expression presented by these authors. In case of the diffuse scattering, (6.12) and (6.13) lead to the following expressions for the thermophoretic and drag forces

$$F_T = -\frac{1}{2\sqrt{\pi}}, \quad (7.1)$$

$$F_u = \frac{4}{3\sqrt{\pi}} \left(1 + \frac{\pi}{8}\right), \quad (7.2)$$

which are well known from the literature, e.g. Takata *et al.* (1993); Beresnev & Chernyak (1995); Sone (2007).

7.2. Transitional regime

Under the assumption of complete accommodation of gas particles on the surface, the results obtained for the thermophoretic and viscous drag forces were compared to those presented by Beresnev & Chernyak (1995); Beresnev *et al.* (1990); Takata & Sone (1992); Takata *et al.* (1993). The comparison is shown in figures 6 and 7, in which F_T^* and F_u^* denote the ratio of the thermophoretic and drag forces to the corresponding values (7.1) and (7.2) in the free molecular regime. Beresnev & Chernyak (1995); Beresnev *et al.* (1990) used the integral-moment method to solve the same linearized kinetic equation of the present work, while Takata & Sone (1992); Takata *et al.* (1993) solved the full linearized Boltzmann equation via a finite difference scheme method and the similarity solution proposed by Sone (1966). It is worth noting that the integral-moment method consists on obtaining a set of integral equations for the moments of the distribution function and its advantage is that only the physical space must be discretized. However, this method requires much more computational memory and CPU time than that required when the discrete velocity method is employed. Regarding the solution of the full Boltzmann equation, in spite of the great computational infrastructure currently available, to find this solution is still a difficult task which requires a great computational effort so that the use of kinetic equations still plays an important role in the solution of

problems of practical interest in the field of rarefied gas dynamics. According to figures (6) and (7), there is a good agreement between our results and those provided by the other authors when diffuse scattering is assumed. The reciprocity relation (5.7) is fulfilled within an accuracy of 0.1%. Table 1 shows the fulfillment of the reciprocity relation (5.7) when $\delta=0.1$ and 1 for some sets of accommodation coefficients.

For other kinds of gas-surface interaction law, some numerical results obtained in the present work are presented in tables (2) and (3) in a range of rarefaction parameter δ which covers the free molecular, transitional and hydrodynamic regimes. The values of the accommodation coefficients considered in the calculations were chosen because, in practice, the coefficients vary in the ranges $0.6 \leq \alpha_t \leq 1$ and $0.1 \leq \alpha_n \leq 1$ for some gases, see e.g. Sharipov (1999); Sharipov & Moldover (2016). According to table 2, the thermophoretic force can be either in the direction of the temperature gradient or in the opposite direction to it. Usually, the thermophoretic force is in the opposite direction to the temperature gradient, i.e. the force tends to move the particle from hot to cold region. However, in some situations the movement of the particle from cold to hot region can occur and such a phenomenon is known as negative thermophoresis, which corresponds to a force in the same direction of the temperature gradient. The negative thermophoresis of particles with high thermal conductivity is expected to appear at large values of rarefaction parameter, i.e. in the continuum and near-continuum regimes. Table 2 shows the existence of negative thermophoresis when $\delta=10$ in case of some sets of accommodation coefficients. For instance, when $\alpha_n=0.1$ and α_t varies from 1 to 0.5, the force is reversed, i.e. the force is positive in the direction of the temperature gradient. Therefore, one can conclude that the occurrence of the negative thermophoresis depends not only on the rarefaction degree of the gas flow and thermal conductivity of aerosol particles, but also on the accommodation coefficients on the surface. Therefore, the appropriate modelling of the gas-surface interaction plays a fundamental role for the correct description of the thermophoresis phenomenon.

According to tables 2 and 3, the thermophoretic and drag forces depend on both accommodation coefficients in the whole range of the gas rarefaction. As one can see in table 2, for fixed values of α_n , when the thermophoretic force is in the opposite direction to the temperature gradient, its magnitude decreases as α_t varies from 1 to 0.5. Moreover, for fixed values of α_t , the magnitude of the thermophoretic force increases when α_n varies from 1 to 0.1. The same qualitative behavior is observed in table 3 for the drag force on the sphere. In fact, this kind of behavior is due to the fact that an increase of α_t means an increase of tangential stress acting on the sphere, while an increase of α_n means an increase of normal stress on the sphere. However, when the force is reversed, the larger α_t and α_n the larger the magnitude of the thermophoretic force acting on the sphere. The results given in these tables also show us that, in spite of the smallness of the thermophoretic force in comparison to the drag force on the sphere, the dependence of the thermophoretic force on the accommodation coefficients is larger than that observed for the drag force. For instance, the maximum deviation of the thermophoretic force from the corresponding value for complete accommodation is around 50% when $\delta=0.1$, 94% when $\delta=1$ and larger than 100% when $\delta=10$. On the other hand, the maximum deviation of the drag force from that value in case of diffuse scattering is around 7% when $\delta=0.1$, 5% when $\delta=1$ and 0.5% when $\delta=10$. It can also be seen that the dependence of the thermophoretic force on the accommodation coefficients is larger in the hydrodynamic regime, while for the drag force such a dependence is larger in the free molecular regime.

7.3. Slip flow regime

In situations where $\delta \gg 1$, the drag force acting on the sphere can be obtained from the solution of the Navier-Stokes equations with slip boundary condition. Thus, according to Sharipov (2011), the dimensionless drag force is written as

$$F_u = \frac{3}{2\delta} \left(1 - \frac{\sigma_P}{\delta} \right), \quad (7.3)$$

where σ_P is the viscous slip coefficient, which strongly depends on the TMAC. Siewert & Sharipov (2002); Sharipov (2003a) provide some values of σ_P for a single gas obtained numerically via the solution of the Shakhov kinetic equation and the Cercignani-Lampis model of gas-surface interaction. For practical applications, a formula which perfectly interpolates the results provided by Siewert & Sharipov (2002); Sharipov (2003a) is presented by Sharipov (2011) as follows

$$\sigma_P = \frac{1.772}{\alpha_t} - 0.754. \quad (7.4)$$

The results obtained from (7.3) are in good agreement with the experimental data found in the literature. For instance, in case of $\alpha_t=1$ and $\delta > 10$, the results obtained from (7.3) agree very well with the experimental data provided by Allen & Raabe (1985); Hutchinson *et al.* (1995) for the drag force on spherical particles of polystyrene latex in air at ambient conditions.

Similarly, for situations where $\delta > 10$, an expression for the thermophoretic force on the sphere can be obtained from the solution of the Navier-Stokes-Fourier equations with slip velocity and temperature jump boundary conditions, e.g. Brock (1962). However, the thermophoretic force predicted from these equations have a large deviation from experimental data for high thermal conductivity particles, e.g. Jacobsen & Brock (1965). This failure is attributed to the fact that the first-order slip solution cannot account for the phenomena arising in the vicinity of the particle, which is a region with large departure from local thermodynamic equilibrium. On the contrary, theories based on higher-order approximation in the Knudsen number, as that proposed by Sone (1966), are able to predict the thermophoretic force on high thermal conductivity particles in the continuum and near continuum or slip flow regimes. However, it is worth mentioning that the solutions obtained from higher order approximations in the Knudsen number rely on the accurate determination of the slip velocity and temperature jump coefficients, and these quantities can be strongly dependent on the accommodation coefficients and intermolecular interaction potential. As pointed out in the review by Sharipov (2011), to obtain more reliable theoretical values of the slip and jump coefficients, numerical methods to solve the Boltzmann equation with a realistic potential of intermolecular interaction and new models of the gas-surface interaction should be developed as well as more experiments should be carried out.

7.4. Flow field

The macroscopic characteristics of the gas flow around the sphere are dependent on the accommodation coefficients. Figures 8-11 show the profiles of the radial and polar components of the bulk velocity, density and temperature deviations from equilibrium, respectively, due to the thermodynamic force X_u , as functions of the distance r/δ , when $\delta=0.1, 1$ and 10 . Similarly, Figures 12-15 show the same profiles, but due to the thermodynamic force X_T . Note that, according to the definitions given in (2.8) and (2.10), the dimensionless distance r/δ corresponds to the ratio of the dimension radial distance r' from the sphere to the radius R_0 of the sphere. The dependence on the TMAC is shown

in Figures 8, 9, 12 and 13 with the NEAC fixed at $\alpha_n=0.1$. The dependence on the NEAC is shown in Figures 10, 11, 14 and 15 with the TMAC fixed at $\alpha_t=1$. The fixed values of α_n and α_t were chosen because, as can be noted in tables 2 and 3, the larger deviations of the thermophoretic and drag forces from those values in case of diffuse scattering occurs when $\alpha_n=0.1$ and $\alpha_t=1$. From figures 8-11, regarding the macroscopic quantities due to the thermodynamic force X_u , one can conclude the following. (i) According to figures 8 and 10, near the sphere the radial component of the bulk velocity tends to decrease while the the polar component tends to increase. This situation corresponds to a decrease in the the bulk velocity of the gas flow due to the presence of the sphere. This qualitative behavior is already known from the literature. However, as one can see from these figures, although the bulk velocity of the gas flow does not depend on the NEAC α_n , theres is a small dependence on the TMAC α_t . (ii) Regarding the number density and temperature of the gas flow around the sphere, according to figures 9 and 11, these quantities always decrease in the vicinity of the sphere. However, while the dependence of the density and temperature deviations on the TMAC is negligible, there is a significant dependence on the NEAC. As one can see in figure 11, when α_n varies from 1 to 0.1, the temperature deviation near the sphere strongly deviates from the corresponding plot for diffuse scattering in the three situations of gas rarefaction considered, i.e. $\delta=0.1$, 1 and 10. The dependence of the density deviation on the NEAC is negligible in the free molecular regime, but it tends to be significant as the gas flow tends to the hydrodynamic regime.

From figures 12-15, regarding the macroscopic quantities due to the thermodynamic force X_T , one can conclude the following. (i) According to figures 12 and 14, the radial and polar components of the bulk velocity depends on both accommodation coefficients. However, the dependence on the TMAC tends to be larger as the gas flow tends to the free molecular regime, while the dependence on the NEAC tends to be larger as the gas flow tends to the hydrodynamic regime. Quantitatively, the dependence on the NEAC is larger than that on the TMAC. Figure 14 shows us that when $\delta=10$, $\alpha_n=\alpha_t=1$, the bulk velocity of the gas in the vicinity of the sphere starts to change direction, which means the starting of the negative thermophoresis due to the thermal creep around the sphere. In order to see the dependence of the bulk velocity of the gas flow due to the temperature gradient on the NEAC as well as the appearance of negative thermophoresis, the the radial and polar components of the bulk velocity as functions of the distance r/δ are given in figure 16 in case of $\delta=10$, α_n fixed at 0.1 and α_t varying from 1 to 0.5. According to this figure, the bulk velocity of the gas flow depends strongly on the NEAC and is even reversed when $\alpha_t < 1$, which means a gas flow in the opposite direction to the temperature gradient, i.e. the negative thermophoresis. (ii) The temperature of the gas flow tends to increase in the vicinity of the sphere in free molecular and transition regimes. However, in the hydrodynamic regime the temperature of the gas decreases near the sphere. The qualitative behavior is the same for arbitrary values of accommodation coefficients, but the influence of the NEAC is larger than that on the TMAC.

7.5. Comparison with experiment

Figure 17 shows the comparison between the results obtained in the present work for the dimension thermophoretic force, in μN , and those provided by Bosworth *et al.* (2016) for a copper sphere in argon gas in a wide range of the gas rarefaction. The experimental apparatus employed by Bosworth *et al.* (2016) consisted on measuring the thermophoretic force acting on a sphere, with radius of about 0.025 m, and fixed in the middle of two 61 cm x 61 cm x 0.9 cm copper plates placed within a vacuum chamber filled with argon gas at ambient temperature and pressure ranging from 13.3 Pa to 0.013

Pa. The distance between the plates was fixed at 40 cm and their temperatures were set up to establish a temperature gradient of 35 K/m between them. However, in rarefied conditions, the profile of the gas temperature between the plates is not linear and there is a temperature jump at the plates. Moreover, the temperature gradient through the gas tends to decrease as the pressure decreases. Therefore, to compare our numerical results with the experimental data provided by Bosworth *et al.* (2016), these effects must be taken into account. Thus, for pressures lower than 1 Pa, the temperature gradient was estimated with basis on the temperature profiles presented by Bosworth *et al.* (2016) in figure 5, which were obtained numerically via the DSMC method. The temperature jump coefficient necessary to estimate the gas temperature at the walls was obtained from the interpolating formula given by Sharipov & Moldover (2016). The numerical calculations were carried out for $\alpha_t=1$ and $\alpha_n=0.9$, values recommended by Sharipov & Moldover (2016) for argon gas at ambient temperature and metallic surface. The viscosity of the gas was obtained from Vogel *et al.* (2010). Thus, according to figure 17, there is a good agreement between the results obtained in the present work and the experimental data provided by Bosworth *et al.* (2016). However, although the negative thermophoresis was detected in the experiment carried out by Bosworth *et al.* (2016), in the present work it was not predicted numerically for the chosen set of the accommodation coefficients. Nonetheless, according to the results presented in table 2, the negative thermophoresis is predicted numerically for some sets of accommodation coefficients when $\delta=10$.

8. Concluding remarks

In the present work, the classical problems of thermophoresis and viscous drag on a sphere with high thermal conductivity were investigated on the basis of the linearized kinetic equation proposed by Shakhov and the Cercignani-Lampis model to the gas-surface interaction law. In the free molecular regime the solutions for both problems were obtained analytically, while in the transitional and hydrodynamic regimes the problems were solved numerically via the discrete velocity method with a proper method to take into account the discontinuity of the distribution function around a convex body. The reciprocity relation between the cross phenomena was obtained and verified numerically within an accuracy of 0.1%. The thermophoretic and drag forces acting on the sphere, as well as the macroscopic characteristics of the gas flow around it, were obtained for some sets of TMAC and NEAC obtained from experiments for monoatomic gases at various surfaces. The results show a strong dependence of the thermophoretic force on both accommodation coefficients, including the appearance of the negative thermophoresis in the hydrodynamic regime as TMAC and the NEAC vary. Moreover, the results show a dependence of the viscous drag force on the accommodation coefficients, but such a dependence is smaller than that observed for the thermophoretic force. Similarly, the flow fields around the sphere also depend on the accommodation coefficients, but the dependence of the quantities due to the thermodynamic force X_u is smaller than that observed for the quantities due to the thermodynamic force X_T . As the gas tends to the hydrodynamic regime, the drag force tends to be independent of the NEAC as predicted by the expression obtained from the Navier-Stokes equations with slip conditions. Regarding the comparison with experimental data, a good agreement was verified for the case of a copper sphere in argon gas and the negative thermophoresis was predicted as dependent of the proper choice of the TMAC and NEAC. According to the results presented in the present work, a better understanding of the transport phenomena of spherical aerosols relies on the correct description of the gas-surface interaction law so that further investigations on this research topic should be carried out,

experimentally and numerically. Moreover, since the data on this topic are still scarce, the results provided in the present work represent a significant contribution towards a better understanding of the phoretic phenomena.

Acknowledgments

The present calculations were carried out at the Laboratório Central de Processamento de Alto Desempenho (LCPAD) of Universidade Federal do Paraná (UFPR, Brazil). The authors acknowledge the Conselho Nacional de Desenvolvimento Científico e Tecnológico (CNPq), grant 304831/2018-2, and the Fundação de Amparo à Pesquisa do Estado de São Paulo (FAPESP), grant 2015/20650-5, for the support of the research.

REFERENCES

- ABRAMOWITZ, M & STEGUN, I A 1972 *Handbook of Mathematical Functions with formulas, graphs and mathematical tables*, 9th edn. New York: Dover Publications Inc.
- ALLEN, M. D. & RAABE, O. G. 1985 Slip correction measurements for solid spherical aerosol particles in an improved Millikan apparatus. *Aerosol Sci. Technol.* **4**, 269–286.
- BAILEY, C. L., BARBER, R. W., EMERSON, D R, LOCKERBY, D A & REESE, J M 2004 A critical review on the drag force on a sphere in the transition flow regime. In *PROCEEDINGS OF THE 24TH INTERNATIONAL SYMPOSIUM ON RAREFIED GAS DYNAMICS*, pp. 743–748.
- BERESNEV, S A & CHERNYAK, V G 1995 Thermophoresis of a spherical particle in a rarefied-gas: Numerical analysis based on the model kinetic equations. *Phys. Fluids* **7** (7), 1743–1756.
- BERESNEV, S A, CHERNYAK, V G & FOMYAGIN, G A 1990 Motion of a spherical-particle in a rarefied-gas. Part 2. Drag and thermal polarization. *J. Fluid Mech.* **219**, 405–421.
- BHATNAGAR, P L, GROSS, E P & KROOK, M A 1954 A model for collision processes in gases. *Phys. Rev.* **94**, 511–525.
- BIRD, G A 1994 *Molecular Gas Dynamics and the Direct Simulation of Gas Flows*. Oxford: Oxford University Press.
- BOSWORTH, R W, VENTURA, A L, KETSDEVER, A D & GIMELSHEIN, S F 2016 Measurement of negative thermophoretic force. *J. Fluid Mech.* **805**, 207–221.
- BROCK, J. R. 1962 On the theory of thermal forces on aerosol particles. *J. Colloid Sciences* **17**, 768–780.
- CERCIGNANI, C 1975 *Theory and Application of the Boltzmann Equation*. Edinburgh: Scottish Academic Press.
- CERCIGNANI, C 1988 *The Boltzmann Equation and its Application*. New York: Springer-Verlag.
- CERCIGNANI, C & LAMPIS, M 1971 Kinetic model for gas-surface interaction. *Transp. Theory and Stat. Phys.* **1**,
- CHERNYAK, V G & SOGRABI, T V 2019 The role of molecule-surface interaction in thermophoresis of an aerosol particle. *J. Aerosol Science* **128**, 62–71.
- CUNNINGHAM, E. 1910 On the velocity of steady fall of spherical particles through fluid medium. *Proc. Royal Society London Series A Math. Phys. Sci.* **83**, 357–365.
- DE GROOT, S R & MAZUR, P 1984 *Non-Equilibrium Thermodynamics*. New York: Dover Publications, Inc.
- EDMONDS, T & HOBSON, J P 1965 A study of thermal transpiration using ultrahigh-vacuum techniques. *J. Vac. Sci. and Technol.* **2** (1), 182–197.
- EPSTEIN, P. S. 1924 On the resistance experienced by spheres in their motion through gases. *Phys. Rev.* **23**, 710–733.
- FERZIGER, J H & KAPER, H G 1972 *Mathematical Theory of Transport Processes in Gases*. Amsterdam: North-Holland Publishing Company.
- GRAD, H 1949 On the kinetic theory of rarefied gases. *Commun. Pure Appl. Math.* **2** (4), 331–407.
- HUTCHINSON, D. K., HARPER, M. H. & FELDER, R. L. 1995 Slip correction measurements for solid spherical particles by modulated light scattering. *Aerosol Sci. Technol.* **22**, 202–212.

- JACOBSEN, S. & BROCK, J. R. 1965 The thermal force on spherical sodium chloride aerosols. *J. Colloid. Sci.* **20**, 544–554.
- KOGAN, M N 1988 Gasdynamics of selectively excited gas. *Izv. AN SSSR. Mech. Zhid. i Gaza* (5), 151–158.
- LANDAU, L D & LIFSHITZ, E M 1989 *Fluid Mechanics*. New York: Pergamon.
- LOYALKA, S K 1992 Thermophoretic force on a single-particle. 1. Numerical solution of the linearized Boltzmann equation. *J. Aerosol. Sci.* **23** (3), 291–300.
- NARIS, S & VALOUGEORGIS, D 2005 The driven cavity flow over the whole range of the Knudsen number. *Phys. Fluids* **17** (9), 097106.
- PADRINO, J C, SPRITTLES, J E & LOCKERBY, D A 2019 Thermophoresis of a spherical particle: modelling through moment-based, macroscopic transport equations. *J. Fluid Mech.* **862**, 312–347.
- PODGURSKY, H H & DAVIS, F N 1961 Thermal transpiration at low pressure. The vapor pressure of xenon below 90 K. *J. Phys. Chem.* **65** (8), 1343–1348.
- SAZHIN, O V, BORISOV, S F & SHARIPOV, F 2001 Accommodation coefficient of tangential momentum on atomically clean and contaminated surfaces. *J. Vac. Sci. Technol. A* **19** (5), 2499–2503, erratum: **20** (3), 957 (2002).
- SEMYONOV, Y G, BORISOV, S F & SUETIN, P E 1984 Investigation of heat transfer in rarefied gases over a wide range of Knudsen numbers. *Int. J. Heat Mass Transfer* **27** (10), 1789–1799.
- SHAKHOV, E M 1967 Boltzmann equation and moment equations in curvilinear coordinates. *Fluid Dynamics* **2** (2), 107–109.
- SHAKHOV, E M 1968 Generalization of the Krook kinetic relaxation equation. *Fluid Dynamics* **3** (5), 95–96.
- SHARIPOV, F 1999 Non-isothermal gas flow through rectangular microchannels. *J. Micromech. Microeng.* **9** (4), 394–401.
- SHARIPOV, F 2003a Application of the Cercignani-Lampis scattering kernel to calculations of rarefied gas flows. II. Slip and jump coefficients. *Eur. J. Mech. B / Fluids* **22**, 133–143.
- SHARIPOV, F 2003b Application of the Cercignani-Lampis scattering kernel to calculations of rarefied gas flows. III. Poiseuille flow and thermal creep through a long tube. *Eur. J. Mech. B / Fluids* **22**, 145–154.
- SHARIPOV, F 2006 Onsager-Casimir reciprocal relations based on the Boltzmann equation and gas-surface interaction law. Single gas. *Phys. Rev. E* **73**, 026110.
- SHARIPOV, F 2010 The reciprocal relations between cross phenomena in boundless gaseous systems. *Physica A* **389**, 3743–3760.
- SHARIPOV, F 2011 Data on the velocity slip and temperature jump on a gas-solid interface. *J. Phys. Chem. Ref. Data* **40** (2), 023101.
- SHARIPOV, F 2016 *Rarefied Gas Dynamics. Fundamentals for Research and Practice*. Berlin: Wiley-VCH.
- SHARIPOV, F & KALEMPA, D 2006 Onsager-Casimir reciprocal relations based on the Boltzmann equation and gas-surface interaction. Gaseous mixtures. *J. Stat. Phys.* **125** (3), 661–675.
- SHARIPOV, F & MOLDOVER, M 2016 Energy accommodation coefficient extracted from acoustic resonator experiments. *J. Vac. Sci. Technol. A* **34** (6), 061604.
- SHARIPOV, F M & SUBBOTIN, E A 1993 On optimization of the discrete velocity method used in rarefied gas dynamics. *Z. Angew. Math. Phys. (ZAMP)* **44**, 572–577.
- SHEN, S F 1967 Parametric representation of gas-surface interaction data and the problem of slip-flow boundary conditions with arbitrary accommodation coefficients. *Entropie* **18**, 135.
- SIEWERT, C E & SHARIPOV, F 2002 Model equations in rarefied gas dynamics: Viscous-slip and thermal-slip coefficients. *Phys. Fluids* **14** (12), 4123–4129.
- SONE, Y 1966 Thermal creep in rarefied gas. *J. Phys. Soc. Jpn* **21**, 1836–1837.
- SONE, Y 1972 Flow induced by thermal stress in rarefied gas. *Phys. Fluids* **15**, 1418–1423.
- SONE, Y 2007 *Molecular Gas Dynamics. Theory, Techniques and Applications*. Boston: Birkhäuser.
- SONE, Y & AOKI, K 1983 A similarity solution of the linearized Boltzmann equation with application to thermophoresis of a spherical particle. *Journal de Mecanique Theorique et Appliquee* **2** (1), 3–12.

- SONE, Y & TAKATA, SH 1992 Discontinuity of the velocity distribution function in a rarefied gas around a convex body and the S layer at the bottom of the Knudsen layer. *Trans. Theory Stat. Phys.* **21** (4-6), 501–530.
- STOKES, G. G. 1845 On the theories of the internal friction of fluids in motion and of the equilibrium and motion of elastic solids. *Trans. Cambridge Philos. Soc.* **8**, 287–319.
- STRUCHTRUP, H & TORRILHON, M 2003 Regularization of Grad’s 13-moment equations: Derivation and linear analysis. *Phys. Fluids* **15**, 2668.
- TAKATA, S & SONE, Y 1995 Flow induced around a sphere with a non-uniform surface temperature in a rarefied gas, with application to the drag and thermal force problem of a spherical particle with an arbitrary thermal conductivity. *Eur. J. Mech. B/Fluids* **14** (4), 487–518.
- TAKATA, S, SONE, Y & AOKI, K 1993 Numerical analysis of a uniform flow of a rarefied gas past a sphere on the basis of the Boltzmann equation for hard-sphere molecules. *Phys. Fluids A* **5** (3), 716–737.
- TAKATA, S, AOKI K & SONE, Y 1992 Thermophoresis of a sphere with a uniform temperature: Numerical analysis of the Boltzmann equation for hard-sphere molecules. In *Rarefied Gas Dynamics: Theory and Simulations* (ed. B D Shizgal & D P Weaver), pp. 626–639. Progress in Astronautics and Aeronautics, Washington: AIAA.
- TORRILHON, M 2010 Slow gas microflow past a sphere: analytical solution based on moment equations. *Phys. Fluids* **22** (072001).
- TROTT, WAYNE M., CASTANEDA, JAIME N., TORCZYNSKI, JOHN R., GALLIS, MICHAEL A. & RADER, DANIEL J. 2011 An experimental assembly for precise measurement of thermal accommodation coefficients. *Rev. Sci. Instrum.* **82** (3), 035120.
- VOGEL, E, JAEGER, B, HELLMANN, R & BICH, E 2010 Ab initio pair potential energy curve for the argon atom pair and thermophysical properties for the dilute argon gas. II. Thermophysical properties for low-density argon. *Mol. Phys.* **108** (24), 3335–3352.
- YAMAMOTO, K. & ISHIHARA, Y. 1988 Thermophoresis of a spherical-particle in a rarefied-gas of a transition regime. *Phys. Fluids* **31** (12), 3618–3624.
- YOUNG, J. B. 2011 Thermophoresis of a Spherical Particle: Reassessment, Clarifications, and New Analysis. *Aerosol Science and Technology* **45**, 927–948.
- ZHENG, F 2002 Thermophoresis of spherical and non-spherical particles: a review of theories and experiments. *Adv. Colloid Interface Sci.* **97** (1-3), 255–278.

α_t	α_n	F_T					
		$\delta \rightarrow 0$		$\delta=0.1$		$\delta=1$	
		Eq. (5.7)	Eq. (6.12) ^a	Eq. (5.7)	Eq. (3.5) ^b	Eq. (5.7)	Eq. (3.5) ^b
1	1	-0.2821	-0.2821	-0.2725	-0.2725	-0.1731	-0.1729
	0.7	-0.3299	-0.3299	-0.3221	-0.3221	-0.2280	-0.2279
	0.5	-0.3596	-0.3596	-0.3530	-0.3530	-0.2643	-0.2642
	0.1	-0.4119	-0.4119	-0.4093	-0.4093	-0.3358	-0.3357
0.5	1	-0.2109	-0.2109	-0.2036	-0.2035	-0.1185	-0.1184
	0.7	-0.2594	-0.2594	-0.2531	-0.2531	-0.1754	-0.1753
	0.5	-0.2887	-0.2887	-0.2840	-0.2840	-0.2129	-0.2128
	0.1	-0.3414	-0.3414	-0.3404	-0.3404	-0.2866	-0.2865
0.1	1	-0.1551	-0.1551	-0.1468	-0.1469	-0.0648	-0.0649
	0.7	-0.2030	-0.2030	-0.1964	-0.1964	-0.1221	-0.1223
	0.5	-0.2326	-0.2326	-0.2273	-0.2273	-0.1603	-0.1601
	0.1	-0.2872	-0.2880	-0.2855	-0.2862	-0.2368	-0.2350

^a Analytical solution in the free molecular regime.

^b Numerical solution due to X_T ($n=T$).

TABLE 1. Thermophoretic force on the sphere: verification of the reciprocity relation.

	α_t	F_T				
		$\alpha_n=0.1$	0.5	0.8	0.9	1.0
$\delta \rightarrow 0^a$	0.5	-0.3414	-0.2887	-0.2434	-0.2273	-0.2109
	0.8	-0.3837	-0.3314	-0.2863	-0.2703	-0.2539
	0.9	-0.3978	-0.3455	-0.3004	-0.2844	-0.2680
	1.0	-0.4119	-0.3596	-0.3145	-0.2985	-0.2821
$\delta=0.01$	0.5	-0.3419	-0.2887	-0.2434	-0.2273	-0.2109
	0.8	-0.3840	-0.3309	-0.2856	-0.2696	-0.2531
	0.9	-0.3981	-0.3450	-0.2996	-0.2836	-0.2672
	1.0	-0.4122	-0.3590	-0.3137	-0.2977	-0.2812
$\delta=0.1$	0.5	-0.3404	-0.2840	-0.2365	-0.2200	-0.2031
	0.8	-0.3817	-0.3255	-0.2785	-0.2613	-0.2444
	0.9	-0.3955	-0.3393	-0.2922	-0.2757	-0.2581
	1.0	-0.4093	-0.3530	-0.3059	-0.2894	-0.2725
$\delta=1$	0.5	-0.2865	-0.2129	-0.1502	-0.1320	-0.1136
	0.8	-0.3165	-0.2445	-0.1894	-0.1633	-0.1455
	0.9	-0.3263	-0.2546	-0.1997	-0.1813	-0.1554
	1.0	-0.3360	-0.2645	-0.2099	-0.1915	-0.1730
$\delta=10$	0.5	-0.0643	-0.0191	0.00663	0.01379	0.02054
	0.8	-0.0661	-0.0296	-0.00769	-0.00146	0.00407
	0.9	-0.0668	-0.0319	-0.0109	-0.00473	0.00072
	1.0	-0.0674	-0.0339	-0.0136	-0.00765	-0.00199

^a Eq. (6.12), free molecular regime.

TABLE 2. Dimensionless thermophoretic force on the sphere.

α_t		F_u				
		$\alpha_n=0.1$	0.5	0.8	0.9	1.0
$\delta \rightarrow 0^a$	0.5	0.9312	0.8979	0.8746	0.8670	0.8596
	0.8	1.0441	1.0107	0.9874	0.9799	0.9724
	0.9	1.0817	1.0483	1.0250	1.0175	1.0100
	1.0	1.1193	1.0859	1.0626	1.0551	1.0477
$\delta=0.01$	0.5	0.9276	0.8940	0.8708	0.8633	0.8559
	0.8	1.0397	1.0062	0.9830	0.9755	0.9681
	0.9	1.0771	1.0436	1.0204	1.0129	1.0055
	1.0	1.1144	1.0810	1.0578	1.0503	1.0429
$\delta=0.1$	0.5	0.8954	0.8631	0.8388	0.8316	0.8245
	0.8	1.0027	0.9707	0.9484	0.9387	0.9316
	0.9	1.0382	1.0063	0.9841	0.9769	0.9671
	1.0	1.0738	1.0419	1.0197	1.0125	1.0054
$\delta=1$	0.5	0.6431	0.6237	0.5836	0.5796	0.5757
	0.8	0.7137	0.6953	0.6824	0.6456	0.6419
	0.9	0.7361	0.7179	0.7052	0.7011	0.6627
	1.0	0.7579	0.7400	0.7275	0.7234	0.7194
$\delta=10$	0.5	0.1318	0.1309	0.1306	0.1305	0.1304
	0.8	0.1397	0.1393	0.1391	0.1391	0.1390
	0.9	0.1403	0.1401	0.1400	0.1399	0.1398
	1.0	0.1436	0.1431	0.1430	0.1430	0.1429

^a Eq. (6.13), free molecular regime.

TABLE 3. Dimensionless viscous drag force on the sphere

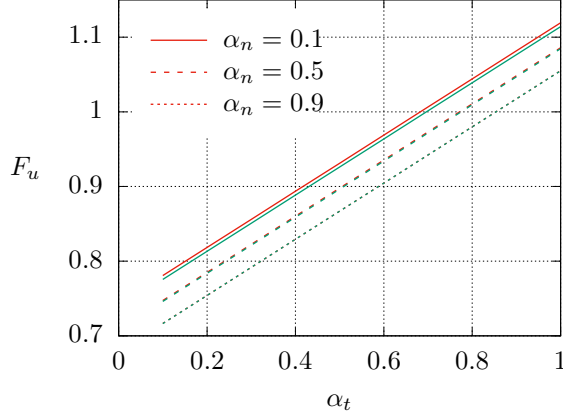


FIGURE 2. Viscous drag force on the sphere in the free molecular regime as function of the tangential momentum accommodation coefficient. Green lines correspond to the results presented by Chernyak & Sograbi (2019). Red lines correspond to the present results.

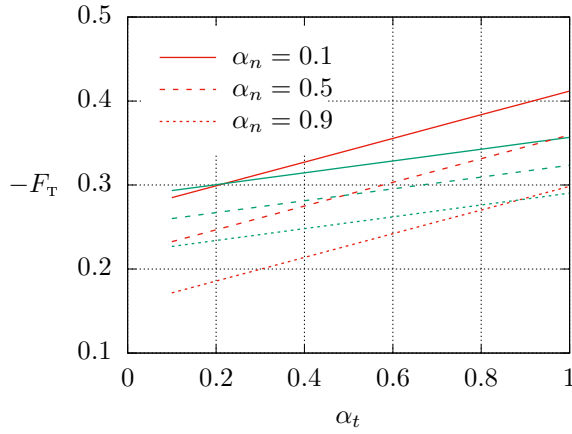


FIGURE 3. Thermophoretic force on the sphere in the free molecular regime as function of the tangential momentum accommodation coefficient. Green lines correspond to the results presented by Chernyak & Sograbi (2019). Red lines correspond to the present results.

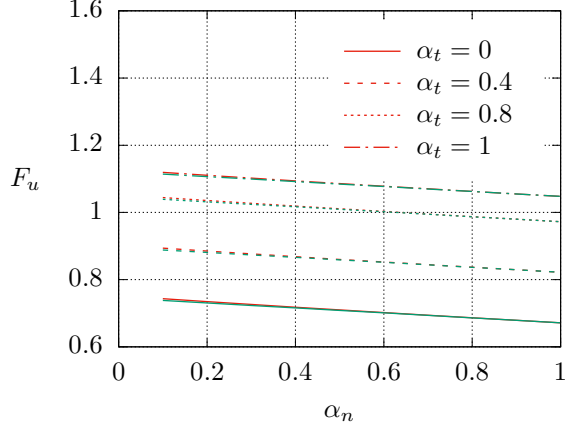


FIGURE 4. Viscous drag force on the sphere in the free molecular regime as function of the normal energy accommodation coefficient. Green lines correspond to the results presented by Chernyak & Sograbi (2019). Red lines correspond to the present results.

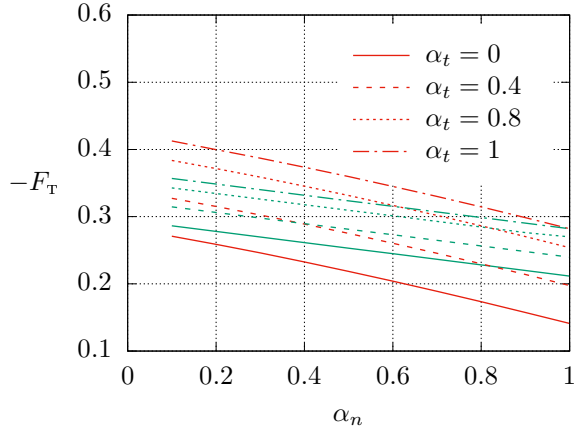


FIGURE 5. Thermophoretic force on the sphere in the free molecular regime as function of the normal energy accommodation coefficient. Green lines correspond to the results presented by Chernyak & Sograbi (2019). Red lines correspond to the present results.

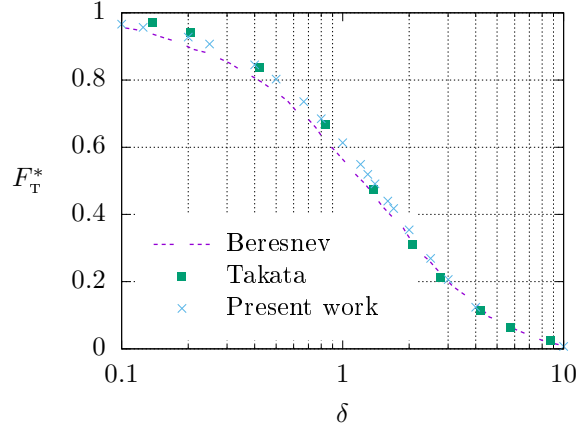


FIGURE 6. Ratio of the thermophoretic force on the sphere to its value in the free molecular regime: comparison to the results presented by Beresnev & Chernyak (1995); Takata & Sone (1992) for diffuse scattering.

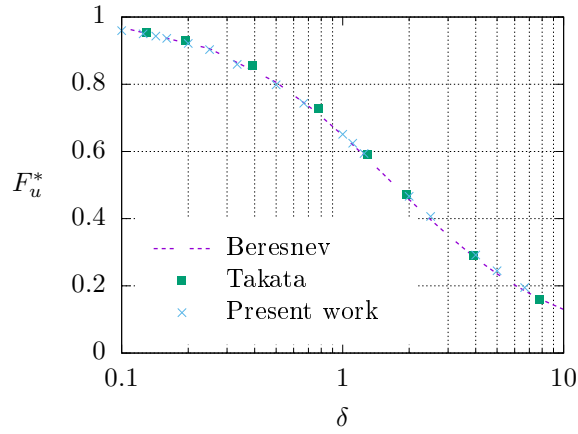


FIGURE 7. Ratio of the drag force on the sphere to its value in the free molecular regime: comparison to the results presented by Beresnev *et al.* (1990); Takata *et al.* (1993) for diffuse scattering.

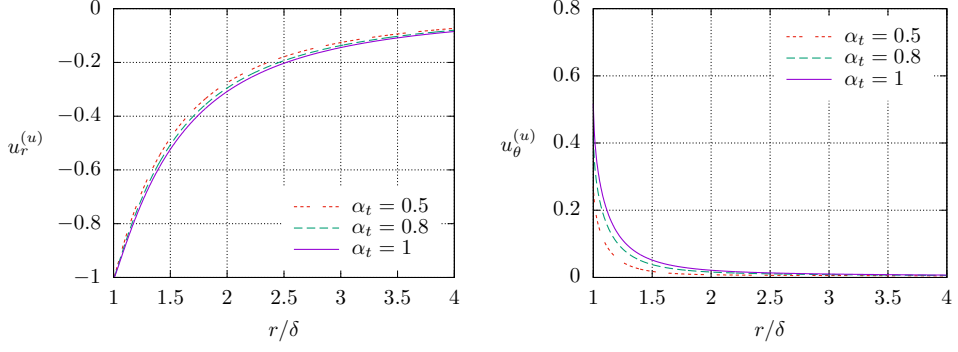
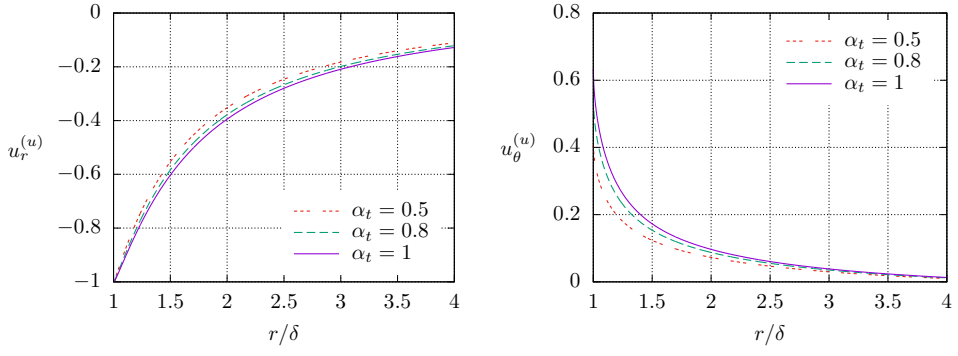
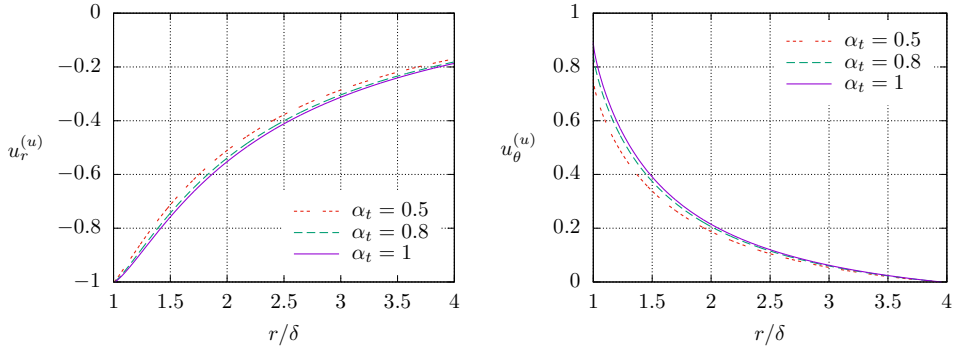
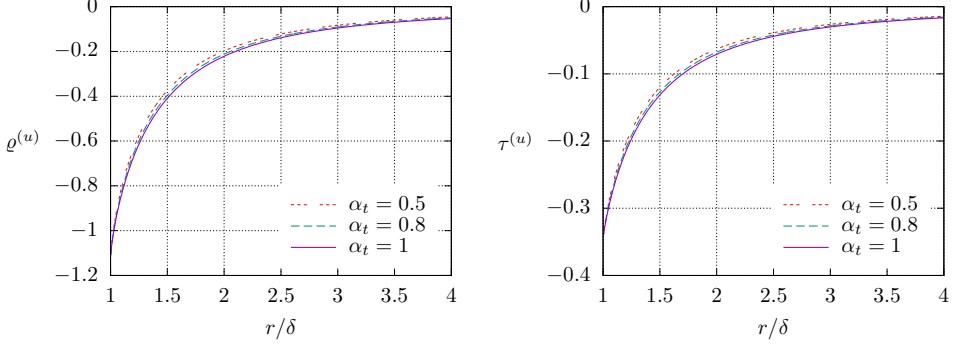
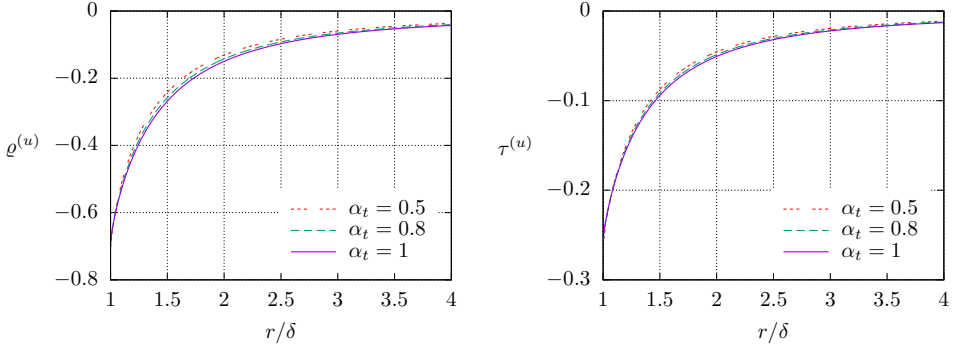
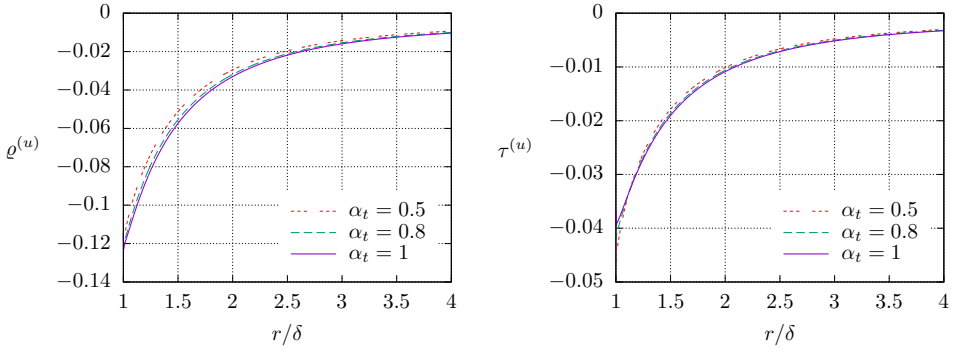
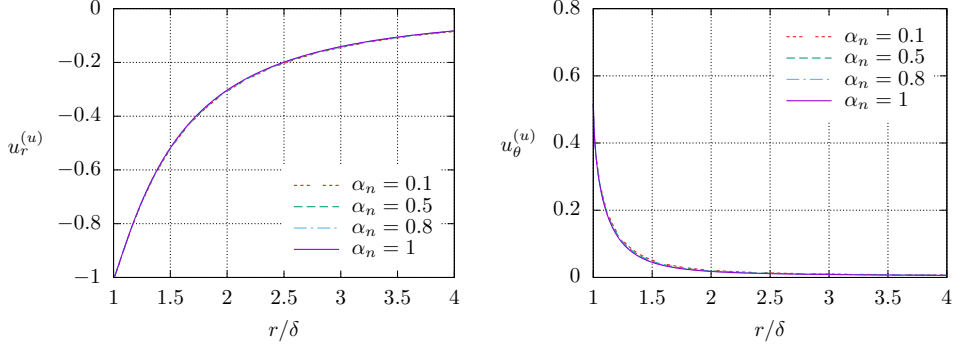
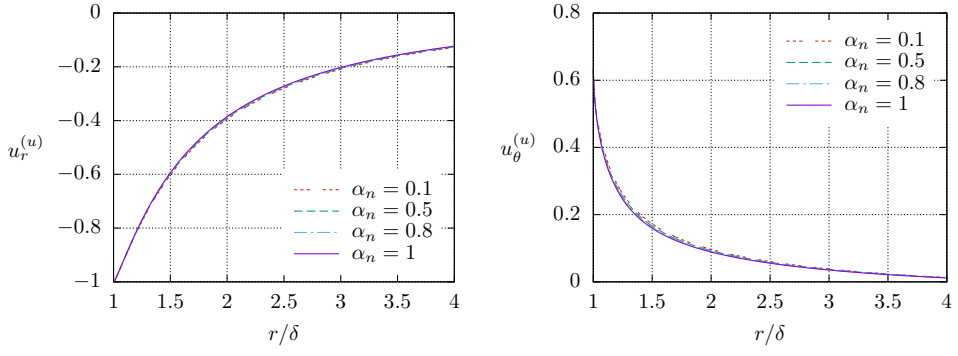
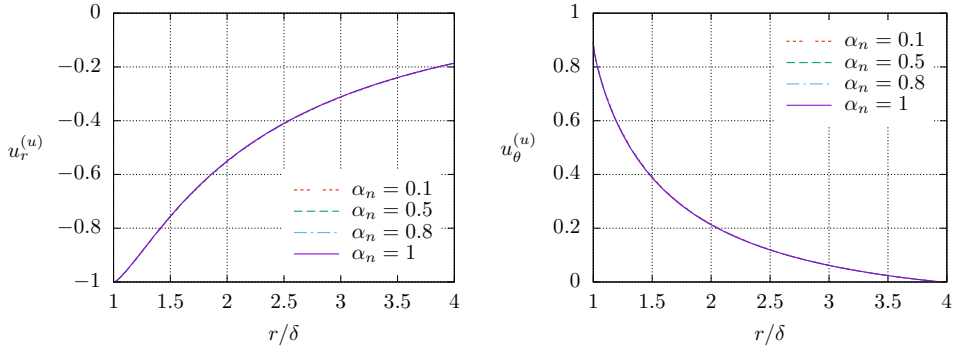
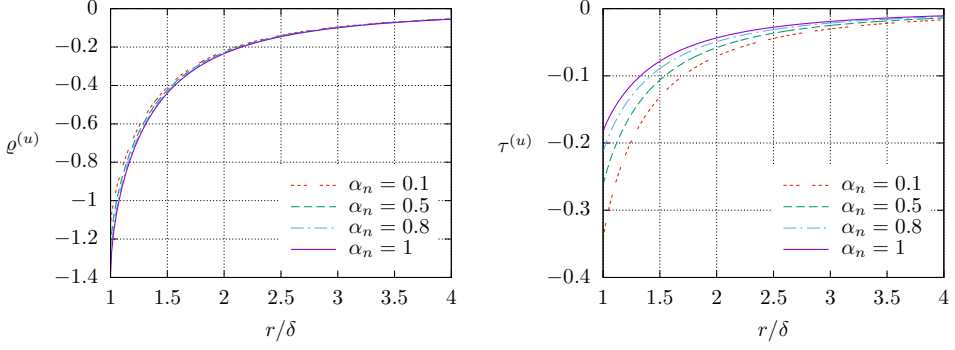
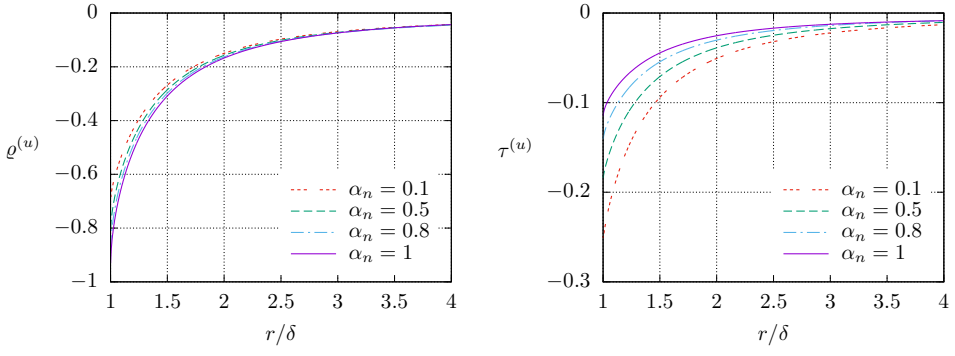
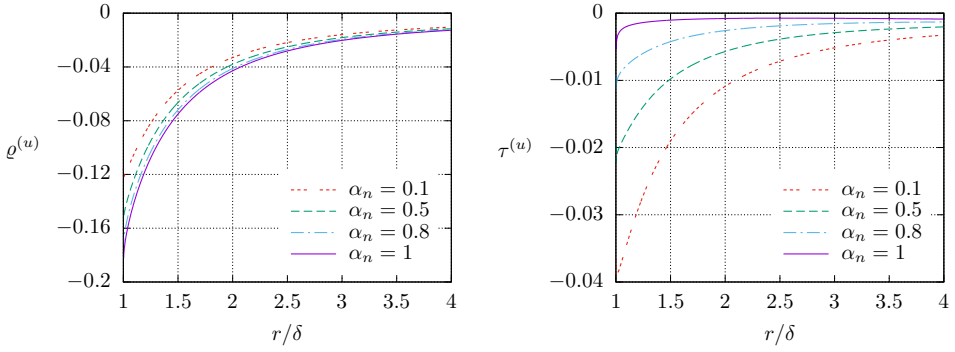
(a) Rarefaction parameter $\delta=0.1$ (b) Rarefaction parameter $\delta=1$ (c) Rarefaction parameter $\delta=10$

FIGURE 8. Components of the bulk velocity as functions of the radial distance from the sphere due to the thermodynamic force X_u for fixed $\alpha_n=0.1$.

(a) Rarefaction parameter $\delta=0.1$ (b) Rarefaction parameter $\delta=1$ (c) Rarefaction parameter $\delta=10$ FIGURE 9. Density and temperature deviations as functions of the radial distance from the sphere due to the thermodynamic force X_u for fixed $\alpha_n=0.1$.

(a) Rarefaction parameter $\delta=0.1$ (b) Rarefaction parameter $\delta=1$ (c) Rarefaction parameter $\delta=10$ FIGURE 10. Components of the bulk velocity as functions of the radial distance from the sphere due to the thermodynamic force X_u for fixed $\alpha_t=1$.

(a) Rarefaction parameter $\delta=0.1$ (b) Rarefaction parameter $\delta=1$ (c) Rarefaction parameter $\delta=10$ FIGURE 11. Density and temperature deviations as functions of the radial distance from the sphere due to the thermodynamic force X_u for fixed $\alpha_t=1$.

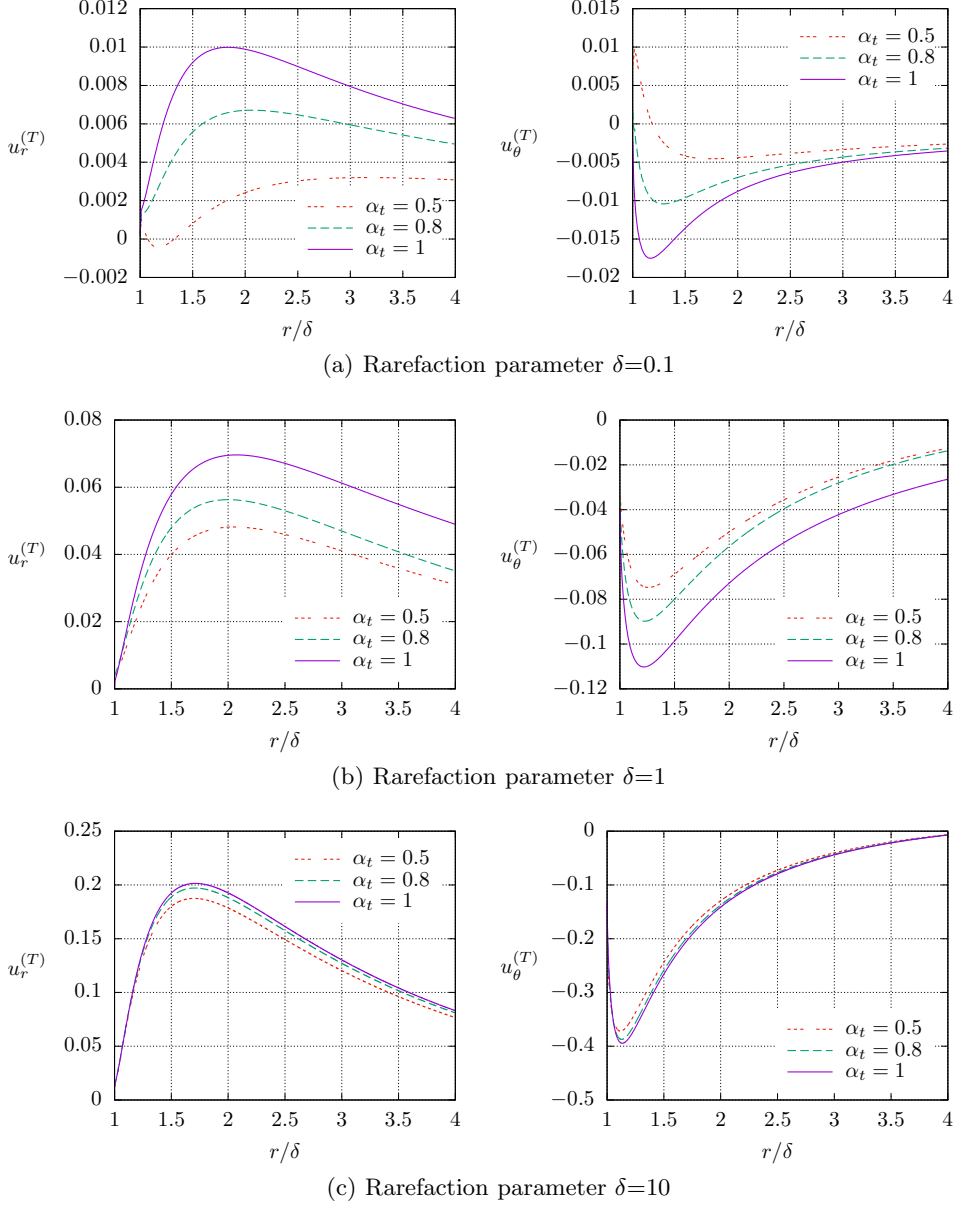


FIGURE 12. Components of the bulk velocity as functions of the radial distance from the sphere due to the thermodynamic force X_T for fixed $\alpha_n=0.1$.

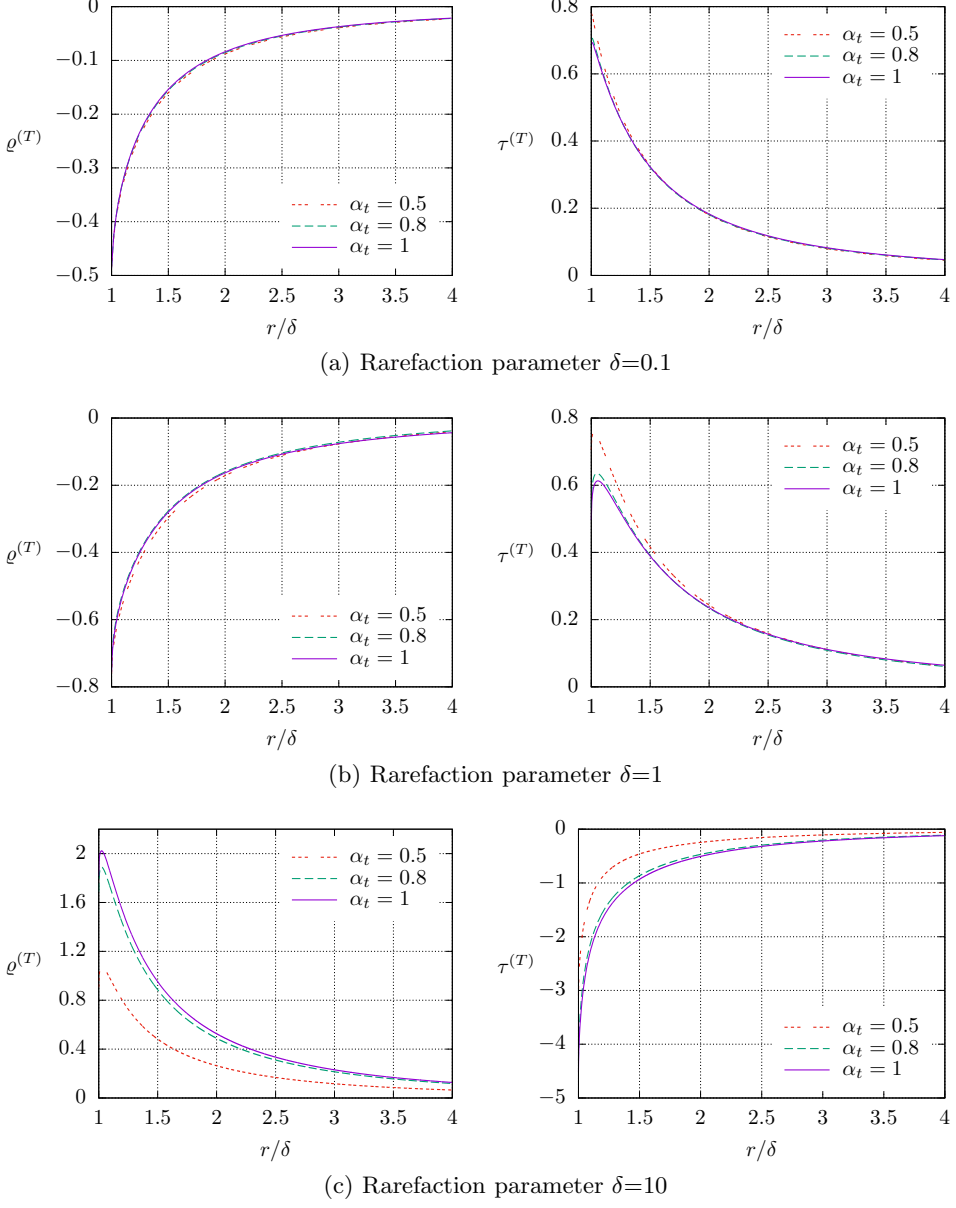


FIGURE 13. Density and temperature deviations as functions of the radial distance from the sphere due to the thermodynamic force X_T for fixed $\alpha_n=0.1$.

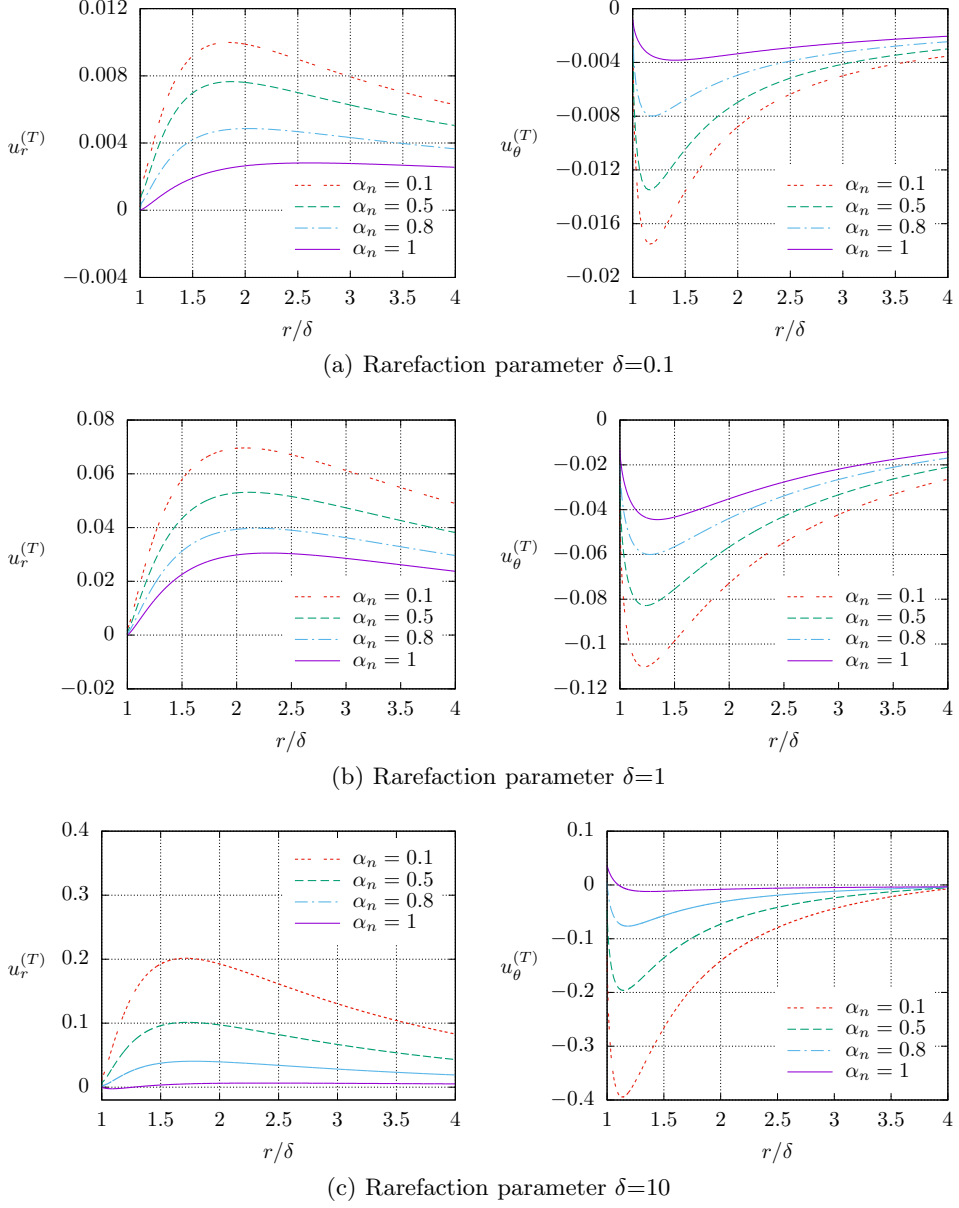
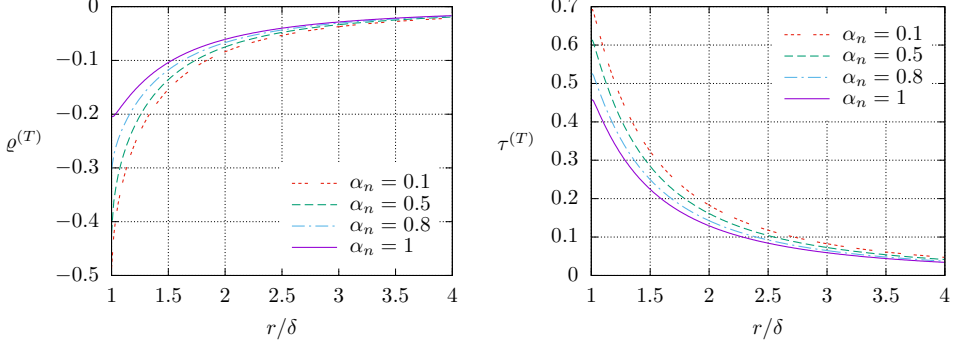
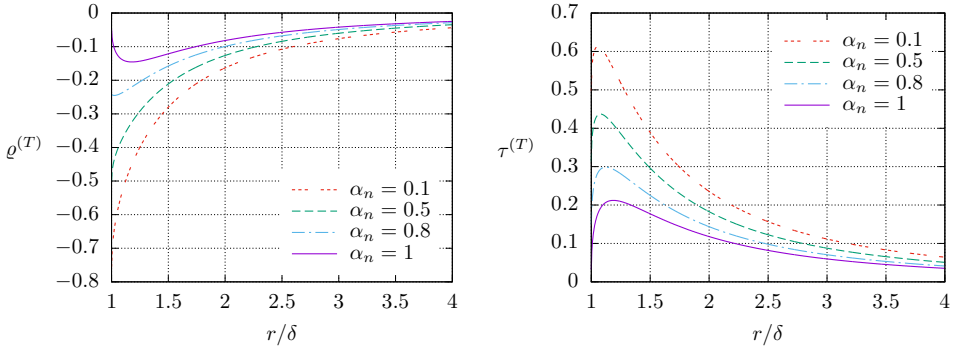
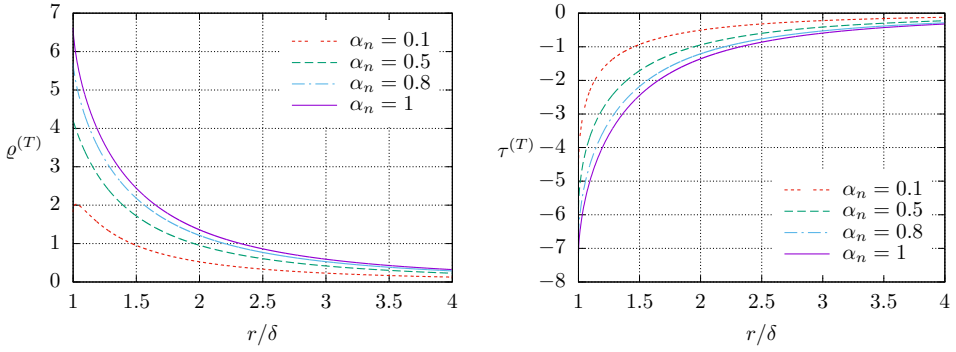


FIGURE 14. Components of the bulk velocity as functions of the radial distance from the sphere due to the thermodynamic force X_T for fixed $\alpha_t=1$.

(a) Rarefaction parameter $\delta=0.1$ (b) Rarefaction parameter $\delta=1$ (c) Rarefaction parameter $\delta=10$ FIGURE 15. Density and temperature deviations as functions of the radial distance from the sphere due to the thermodynamic force X_T for fixed $\alpha_t=1$.

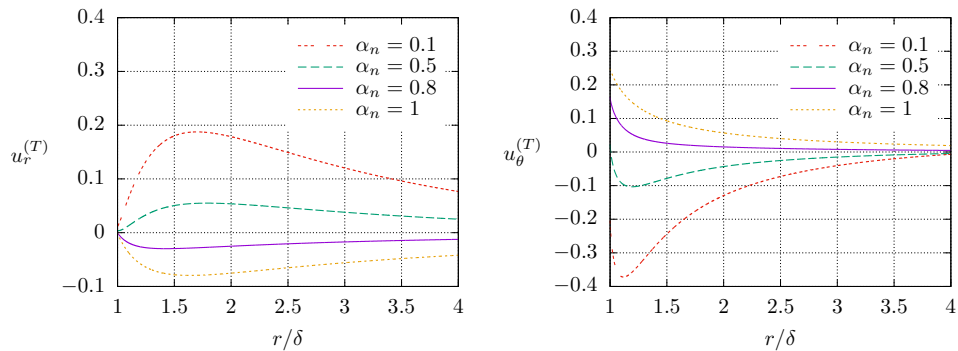


FIGURE 16. Components of the bulk velocity as functions of the radial distance from the sphere due to thermodynamic force X_T for fixed $\alpha_t=0.5$ and $\delta=10$.

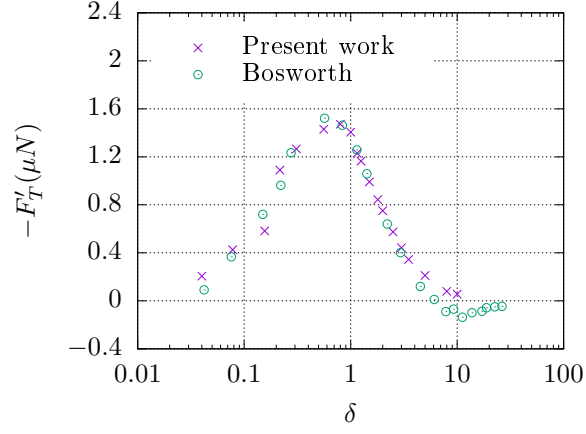


FIGURE 17. Dimensionless thermophoretic force: comparison with experimental data provided by Bosworth *et al.* (2016) for a copper sphere in argon gas.